Critical behavior of the energy and pressure correlation functions in SU(2) gauge theory

C. Pica

in collaboration with

F. Karsch and K. Hübner

Brookhaven National Lab

LATTICE 2008 - 7/17/2008

Outline

1 Introduction

2 SU(2) thermodynamics

3 Correlation functions

4 Conclusions

Motivation

The experimental evidence for rapid thermalization of the dense matter created in heavy ion collisions at RHIC has led to the interpretation of the quark gluon plasma above but close to the transition temperature as a strongly interacting medium that has properties of an almost perfect liquid.

These experimental findings also renewed the interest in determining transport properties of gauge theories through the calculation of correlation functions of the energy-momentum tensor on the lattice.

Recently it has been argued that close to the transition from low temperature hadronic matter to the plasma phase of QCD bulk viscosity might play a much more important role than shear viscosity [Kharzeev&Tuchin(2007)].

The singular behavior of bulk viscosity in the vicinity of a critical point has long been known in statistical physics. In particular, at the critical point of the liquid gas transition it has been argued that the divergence of ζ is strong and, in fact, almost quadratic in the inverse reduced temperature t. The singular behavior, $\zeta \sim t^{-z\nu+\alpha}$, with α, ν denoting static critical exponents of the 3-d Ising model and z being a dynamical exponent characterizing the equilibration of density fluctuations, goes along with a strong divergence of the relaxation time for density fluctuations, τ_R. Their ratio, $\zeta/\tau_R \sim t^{\alpha}$, however, is proportional to the inverse of the specific heat and thus vanishes slowly at the critical point.

The SU(2) gauge theory with its second order deconfinement phase transition seems to be an ideal model to explore critical behavior of dynamical properties, e.g. transport coefficients.

Motivation

The experimental evidence for rapid thermalization of the dense matter created in heavy ion collisions at RHIC has led to the interpretation of the quark gluon plasma above but close to the transition temperature as a strongly interacting medium that has properties of an almost perfect liquid.

These experimental findings also renewed the interest in determining transport properties of gauge theories through the calculation of correlation functions of the energy-momentum tensor on the lattice.

Recently it has been argued that close to the transition from low temperature hadronic matter to the plasma phase of QCD bulk viscosity might play a much more important role than shear viscosity [Kharzeev&Tuchin(2007)].

The singular behavior of bulk viscosity in the vicinity of a critical point has long been known in statistical physics. In particular, at the critical point of the liquid gas transition it has been argued that the divergence of ζ is strong and, in fact, almost quadratic in the inverse reduced temperature t. The singular behavior, $\zeta \sim t^{-z\nu+\alpha}$, with α, ν denoting static critical exponents of the 3-d Ising model and z being a dynamical exponent characterizing the equilibration of density fluctuations, goes along with a strong divergence of the relaxation time for density fluctuations, τ_R. Their ratio, $\zeta/\tau_R \sim t^{\alpha}$, however, is proportional to the inverse of the specific heat and thus vanishes slowly at the critical point.

The SU(2) gauge theory with its second order deconfinement phase transition seems to be an ideal model to explore critical behavior of dynamical properties, e.g. transport coefficients.

Motivation

The experimental evidence for rapid thermalization of the dense matter created in heavy ion collisions at RHIC has led to the interpretation of the quark gluon plasma above but close to the transition temperature as a strongly interacting medium that has properties of an almost perfect liquid.

These experimental findings also renewed the interest in determining transport properties of gauge theories through the calculation of correlation functions of the energy-momentum tensor on the lattice.

Recently it has been argued that close to the transition from low temperature hadronic matter to the plasma phase of QCD bulk viscosity might play a much more important role than shear viscosity [Kharzeev&Tuchin(2007)].

The singular behavior of bulk viscosity in the vicinity of a critical point has long been known in statistical physics. In particular, at the critical point of the liquid gas transition it has been argued that the divergence of ζ is strong and, in fact, almost quadratic in the inverse reduced temperature t. The singular behavior, $\zeta \sim t^{-z\nu+\alpha}$, with α, ν denoting static critical exponents of the 3-d Ising model and z being a dynamical exponent characterizing the equilibration of density fluctuations, goes along with a strong divergence of the relaxation time for density fluctuations, τ_R. Their ratio, $\zeta/\tau_R \sim t^{\alpha}$, however, is proportional to the inverse of the specific heat and thus vanishes slowly at the critical point.

The SU(2) gauge theory with its second order deconfinement phase transition seems to be an ideal model to explore critical behavior of dynamical properties, e.g. transport coefficients.

Motivation

The experimental evidence for rapid thermalization of the dense matter created in heavy ion collisions at RHIC has led to the interpretation of the quark gluon plasma above but close to the transition temperature as a strongly interacting medium that has properties of an almost perfect liquid.

These experimental findings also renewed the interest in determining transport properties of gauge theories through the calculation of correlation functions of the energy-momentum tensor on the lattice.

Recently it has been argued that close to the transition from low temperature hadronic matter to the plasma phase of QCD bulk viscosity might play a much more important role than shear viscosity [Kharzeev&Tuchin(2007)].

The singular behavior of bulk viscosity in the vicinity of a critical point has long been known in statistical physics. In particular, at the critical point of the liquid gas transition it has been argued that the divergence of ζ is strong and, in fact, almost quadratic in the inverse reduced temperature t. The singular behavior, $\zeta \sim t^{-z\nu+\alpha}$, with $\alpha,\ \nu$ denoting static critical exponents of the 3-d Ising model and z being a dynamical exponent characterizing the equilibration of density fluctuations, goes along with a strong divergence of the relaxation time for density fluctuations, τ_R. Their ratio, $\zeta/\tau_R \sim t^{\alpha}$, however, is proportional to the inverse of the specific heat and thus vanishes slowly at the critical point.

The SU(2) gauge theory with its second order deconfinement phase transition seems to be an ideal model to explore critical behavior of dynamical properties, e.g. transport coefficients.

Motivation

The experimental evidence for rapid thermalization of the dense matter created in heavy ion collisions at RHIC has led to the interpretation of the quark gluon plasma above but close to the transition temperature as a strongly interacting medium that has properties of an almost perfect liquid.

These experimental findings also renewed the interest in determining transport properties of gauge theories through the calculation of correlation functions of the energy-momentum tensor on the lattice.

Recently it has been argued that close to the transition from low temperature hadronic matter to the plasma phase of QCD bulk viscosity might play a much more important role than shear viscosity [Kharzeev&Tuchin(2007)].

The singular behavior of bulk viscosity in the vicinity of a critical point has long been known in statistical physics. In particular, at the critical point of the liquid gas transition it has been argued that the divergence of ζ is strong and, in fact, almost quadratic in the inverse reduced temperature t. The singular behavior, $\zeta \sim t^{-z\nu+\alpha}$, with $\alpha,\ \nu$ denoting static critical exponents of the 3-d Ising model and z being a dynamical exponent characterizing the equilibration of density fluctuations, goes along with a strong divergence of the relaxation time for density fluctuations, τ_R. Their ratio, $\zeta/\tau_R \sim t^{\alpha}$, however, is proportional to the inverse of the specific heat and thus vanishes slowly at the critical point.

The SU(2) gauge theory with its second order deconfinement phase transition seems to be an ideal model to explore critical behavior of dynamical properties, e.g. transport coefficients.

Energy-Momentum tensor and bulk viscosity

We indicate with $\Theta^{\mu\nu}$ the energy-momentum tensor. The energy density is $\epsilon = \Theta^{00}$, and the pressure is given by $3p = -\Theta^{ii}$.

Given a zero-momentum connected correlation function at finite temperature T:

$$G_{XY}(\tau, T) = \int d^3x \langle X(\vec{x}, \tau) Y(\vec{0}, 0) \rangle_T \ ,$$

its spectral function ρ_{XY} is given by:

$$G_{XY}(\tau, T) = \int d\omega \rho_{XY}(\omega, T) \cosh[\omega(\tau - 1/2T)] \mathrm{cosech}(\omega/2T) \ .$$

The bulk viscosity can be extracted from the low frequency behavior of the spectral function of the pressure-pressure correlator:

$$\zeta(T) = \pi \lim_{\omega \to 0} \frac{\rho_{pp}(\omega, T)}{\omega} \ .$$

Outline

1 Introduction

2 SU(2) thermodynamics

3 Correlation functions

4 Conclusions

Differential formalism

Define the action on an anisotropic lattice as:

$$S = \frac{2N}{g_\sigma^2} \sum_{x,i>j=1,2,3} \left(1 - \frac{1}{N}\mathrm{ReTrP_{ij}(x)}\right) + \frac{2N}{g_\tau^2} \sum_{x,j=1,2,3} \left(1 - \frac{1}{N}\mathrm{ReTrP_{4j}(x)}\right) \quad .$$

Thermodynamic quantities can be obtained taking derivatives of the free energy, e.g.:

$$\begin{aligned} \epsilon &= -\frac{1}{V}\frac{\partial \ln Z}{\partial(1/T)} - \epsilon_0 \\ p &= T\frac{\partial \ln Z}{\partial V} - P_0 \quad , \end{aligned}$$

where we have subtracted the vacuum contribution of T=0.

Differential formalism

On an isotropic lattice these are:

$$\begin{aligned}
\frac{\epsilon}{T^4} &= NN_\tau^4 \left\{ 3\left[2g^{-2} - (c_\sigma - c_\tau)\right](P_\sigma - P_\tau) + 3\left[c_\sigma + c_\tau\right](2P_0 - P_\sigma - P_\tau) \right\} \\
\frac{p}{T^4} &= NN_\tau^4 \left\{ \left[2g^{-2} - (c_\sigma - c_\tau)\right](P_\sigma - P_\tau) - 3\left[c_\sigma + c_\tau\right](2P_0 - P_\sigma - P_\tau) \right\} \\
\frac{s}{T^3} = \frac{\epsilon + p}{T^4} &= 4NN_\tau^4 \left[2g^{-2} - (c_\sigma - c_\tau)\right](P_\sigma - P_\tau) \\
\frac{\Theta^{\mu\mu}}{T^4} = \frac{\epsilon - 3p}{T^4} &= 12NN_\tau^4 \left[c_\sigma + c_\tau\right](2P_0 - P_\sigma - P_\tau)
\end{aligned}$$

where

$$g^{-2} = g_\sigma^{-2} = g_\tau^{-2}; \quad B(g^{-2}) \equiv \left.\frac{dg^{-2}}{d\ln a}\right|_{\xi=1} = -2\left(c_\sigma + c_\tau\right); \quad c_{\sigma,\tau} = \left.\frac{\partial g_{\sigma,\tau}^{-2}}{\partial \xi}\right|_{\xi=1}$$

$$P_\sigma = \frac{1}{3N_\sigma^3 N_\tau} \sum_{x,i>j=1,2,3} \left(1 - \frac{1}{N}\mathrm{ReTrP_{ij}(x)}\right); \quad P_\tau = \frac{1}{3N_\sigma^3 N_\tau} \sum_{x,j=1,2,3} \left(1 - \frac{1}{N}\mathrm{ReTrP_{4j}(x)}\right)$$

Critical energy density and pressure

As check of our setup we perform a finite-size scaling analysis of ϵ and p at the critical point.
From the scaling ansatz for the singular part of the free energy density f ($t \equiv (T - T_c)/T_c$):

$$f_s(t, L^{-1}) = b^{-d} f_s(t b^{y_t}, L^{-1} b)$$

it follows for the energy density and pressure ($\nu = 1/y_t$, $\alpha = 2 - d\nu$):

$$\left(\frac{p(T_c)}{T_c^4}\right)_{N_\tau, N_\sigma} = \left(\frac{p(T_c)}{T_c^4}\right)_{N_\tau, \infty} + a_p N_\sigma^{-3} ,$$

$$\left(\frac{\epsilon(T_c)}{T_c^4}\right)_{N_\tau, N_\sigma} = \left(\frac{\epsilon(T_c)}{T_c^4}\right)_{N_\tau, \infty} + a_\epsilon N_\sigma^{-(1-\alpha)/\nu} .$$

The critical exponents $\alpha = 0.110(1)$ and $\nu = 0.6301(4)$ are known from the 3d Ising model.

From the critical behavior of ϵ and p it follows that for generic combinations of the two, like $\epsilon - 3p$ and $\epsilon + p$, will have the same volume scaling as the energy density.
Note also that the value of P_0, entering in the above expressions, is inessential in the analisys of finite-size scaling at fixed N_τ, since it can be considered as a constant.

Critical energy density and pressure

We used lattices with $N_\tau = 4, 6, 8$ and N_σ / N_τ up to 24 ($96^3 \times N_\tau$). The infinite volume critical couplings are already known:

$$N_\tau = 4 \quad \beta_c = 2.29895(10) \quad [\textit{Engels\&Scheideler}(1999)]$$
$$N_\tau = 6 \quad \beta_c = 2.4265(30) \quad [\textit{Engels}, \textit{Fingberg\&Miller}(1992)]$$
$$N_\tau = 8 \quad \beta_c = 2.5115(40) \quad [\textit{Fingberg}, \textit{Heller\&Karsch}(1993)]$$

Critical energy density and pressure

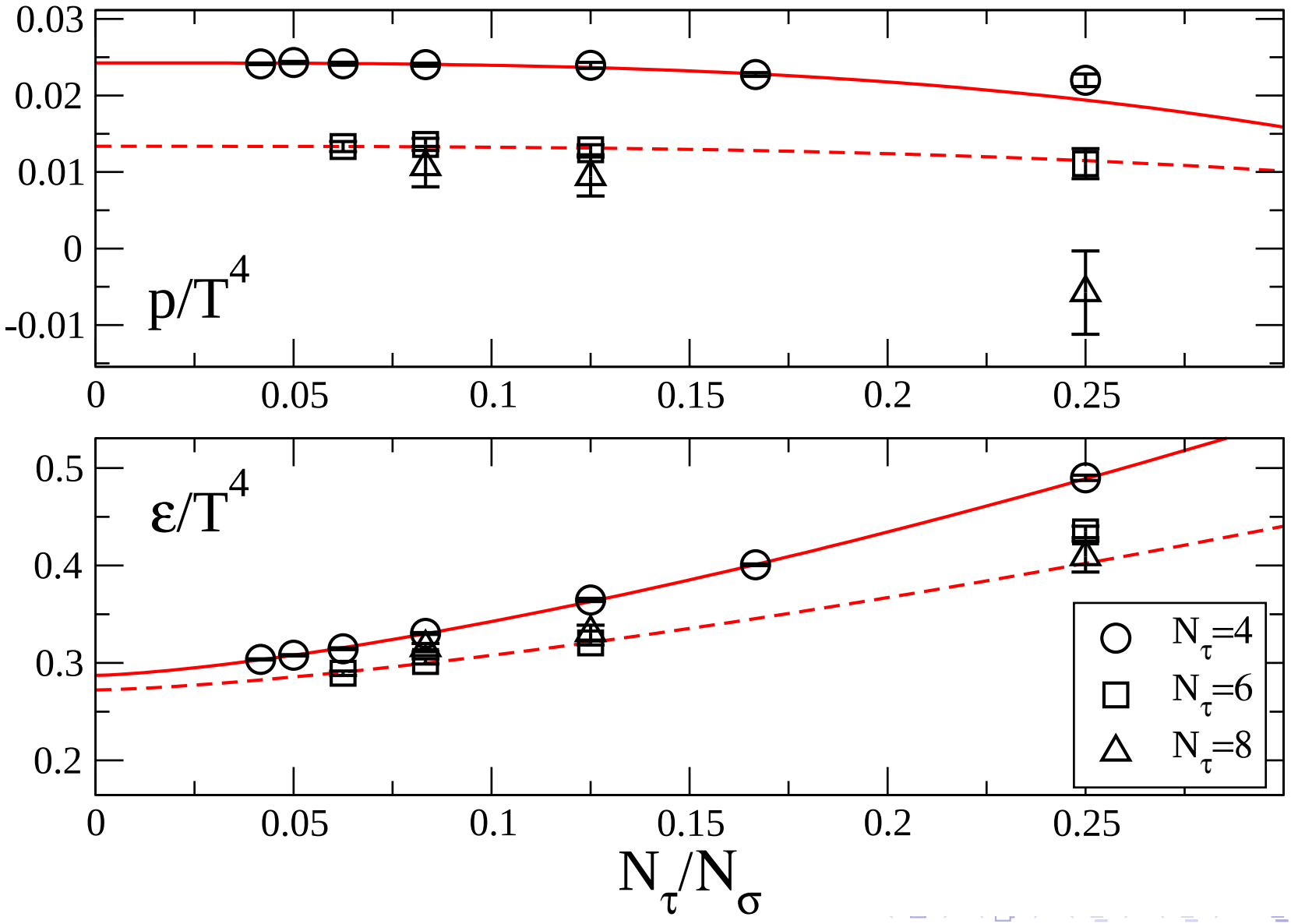

Critical energy density and pressure

To check the universality class, using the $N_\tau = 4$ lattices, where more volumes are available, we determined the critical exponent $(1-\alpha)/\nu$ by a fit to the expected functional form of the energy density.
The fit yields $(1-\alpha)/\nu = 1.41(6)$ in agreement with $(1-\alpha)/\nu = 1.412(1)$ for Ising 3d.

Using the known values for the critical exponents, we extracted the infinite volume critical ϵ and p. The fit was done fixing the known value of the critical exponents and using only lattices with $N_\sigma/N_\tau > 4$.

N_τ	$\epsilon(T_c)/T_c^4$	$P(T_c)/T_c^4$
4	0.28724(53)	0.02423(30)
6	0.2722(31)	0.0135(8)
8	–	0.0107(15)

The result for $\epsilon(T_c)/T_c^4$ is compatible with the value $\epsilon(T_c)/T_c^4 = 0.256(23)$ from [Engels,Karsch&Redlich(1995)].

The result for the critical pressure is new.

Outline

1 Introduction

2 SU(2) thermodynamics

3 Correlation functions

4 Conclusions

Correlation function of $\Theta^{\mu\mu}$

The correlation function for the trace of the energy-momentum tensor can be decomposed as:

$$G_{\Theta\Theta}(\tau, T) = G_{\epsilon\epsilon}(\tau, T) - 6G_{\epsilon p}(\tau, T) + 9G_{pp}(\tau, T) \ .$$

The correlation functions involving the energy density operator $G_{\epsilon Y}(\tau, T)$ are independent of τ in the continuum limit. This is easily seen since

$$\langle H(\tau)Y(0)\rangle_T = \frac{1}{Z}\mathrm{Tr}\left[e^{-H/T}H(\tau)Y(0)\right]$$

is independent on time. It also follows that:

$$G_{\epsilon Y}(\tau, T) = -\frac{\partial}{\partial(1/T)}\langle Y\rangle_T \ .$$

Correlation function of $\Theta^{\mu\mu}$

The correlation function for the trace of the energy-momentum tensor can be decomposed as:

$$G_{\Theta\Theta}(\tau, T) = G_{\epsilon\epsilon}(\tau, T) - 6G_{\epsilon p}(\tau, T) + 9G_{pp}(\tau, T) \ .$$

The whole τ dependence of $G_{\Theta\Theta}$ is thus expected to arise from the pressure-pressure correlations.

On the other hand, the dominant temperature dependence comes from the energy-energy correlator, which is proportional to the specific heat:

$$\frac{G_{\epsilon\epsilon}(\tau, T)}{T^5} \sim \frac{c_V}{T^3} \ .$$

At non-zero lattice spacing the direct relation between correlation functions involving the energy operator and temperature derivatives of any observable is violated by cut-off effects. Nonetheless we expect that these are small in the vicinity of a second order phase transition. One thus may expect that at least the singular behavior of correlation functions that involve correlations with the energy operator will be independent of Euclidean time.

Correlation function of $\Theta^{\mu\mu}$

The correlation function for the trace of the energy-momentum tensor can be decomposed as:

$$G_{\Theta\Theta}(\tau, T) = G_{\epsilon\epsilon}(\tau, T) - 6G_{\epsilon p}(\tau, T) + 9G_{pp}(\tau, T) \ .$$

Close to the deconfinement transition we therefore expect that $G_{\Theta\Theta}$ will show, for every τ, a critical behavior that coincides with that of the specific heat in a 3-dimensional Ising model:

$$\frac{G_{\Theta\Theta}(\tau, T)}{T^5} \sim \frac{c_V}{T^3} \sim A_\pm \left|\frac{T - T_c}{T_c}\right|^{-\alpha} \left(1 + B_\pm \left|\frac{T - T_c}{T_c}\right|^{\omega} + \ldots\right) \quad \text{for} \quad T \to T_c^\pm \ .$$

α	ν	ω/ν	A_+/A_-
0.110(1)	0.6301(4)	0.84(4)	0.54(1)

Like α, also the amplitudes ratio A_+/A_- and the correction to scaling exponent ω are universal.

Critical behavior of $G_{\Theta\Theta}$ – simulation details

We have calculated the correlation function $G_{\Theta\Theta}(\tau, T)$ close to the deconfinement transition point of the SU(2) gauge theory. In our simulation we use lattices of size $N_\sigma^3 N_\tau$ with $N_\tau = 4$. This gives us information on the correlation function at two non-zero values of Euclidean time, *i.e.* at $\tau T = 1/4$ and at the midpoint $\tau T = 1/2$.

Most of our simulations have been performed at temperatures close to the phase transition where the correlation length becomes large. This required calculations on large spatial lattices in order to eliminate finite volume effects.

We used spatial lattice sizes with aspect ratios N_σ / N_τ varying from 8 ($32^3 \times 4$ lattices) up to values as large as 32 ($128^3 \times 4$ lattices).

A large number of configurations are required to reach the statistical accuracy – $\mathcal{O}(5\%)$ at $\tau T = 1/2$ – needed for scaling test near the critical point. We have generated about $1 \cdot 10^6$ configurations on our smaller lattices and up to $4 \cdot 10^5$ on the large lattices.

The algorithm used to generate the configurations uses a standard mixture of heat-bath and over-relation updates in a typical ratio of 1:4-1:6 to keep correlations between consecutive configurations small. Autocorrelation times in the transition region range from $\mathcal{O}(1)$ on the small lattices to about 40 on the largest lattices.

Numerical simulations have been performed on the BlueGene/L, BlueGene/P at the New York Center for Computational Science (NYCCS), using a code developed specifically for this work.

Critical behavior of $G_{\Theta\Theta}$ – simulation details

We have calculated the correlation function $G_{\Theta\Theta}(\tau, T)$ close to the deconfinement transition point of the SU(2) gauge theory. In our simulation we use lattices of size $N_\sigma^3 N_\tau$ with $N_\tau = 4$. This gives us information on the correlation function at two non-zero values of Euclidean time, *i.e.* at $\tau T = 1/4$ and at the midpoint $\tau T = 1/2$.

Most of our simulations have been performed at temperatures close to the phase transition where the correlation length becomes large. This required calculations on large spatial lattices in order to eliminate finite volume effects.

We used spatial lattice sizes with aspect ratios N_σ / N_τ varying from 8 ($32^3 \times 4$ lattices) up to values as large as 32 ($128^3 \times 4$ lattices).

A large number of configurations are required to reach the statistical accuracy – $\mathcal{O}(5\%)$ at $\tau T = 1/2$ – needed for scaling test near the critical point. We have generated about $1 \cdot 10^6$ configurations on our smaller lattices and up to $4 \cdot 10^5$ on the large lattices.

The algorithm used to generate the configurations uses a standard mixture of heat-bath and over-relation updates in a typical ratio of 1:4-1:6 to keep correlations between consecutive configurations small. Autocorrelation times in the transition region range from $\mathcal{O}(1)$ on the small lattices to about 40 on the largest lattices.

Numerical simulations have been performed on the BlueGene/L, BlueGene/P at the New York Center for Computational Science (NYCCS), using a code developed specifically for this work.

Critical behavior of $G_{\Theta\Theta}$ – simulation details

We have calculated the correlation function $G_{\Theta\Theta}(\tau, T)$ close to the deconfinement transition point of the SU(2) gauge theory. In our simulation we use lattices of size $N_\sigma^3 N_\tau$ with $N_\tau = 4$. This gives us information on the correlation function at two non-zero values of Euclidean time, *i.e.* at $\tau T = 1/4$ and at the midpoint $\tau T = 1/2$.

Most of our simulations have been performed at temperatures close to the phase transition where the correlation length becomes large. This required calculations on large spatial lattices in order to eliminate finite volume effects.

We used spatial lattice sizes with aspect ratios N_σ / N_τ varying from 8 ($32^3 \times 4$ lattices) up to values as large as 32 ($128^3 \times 4$ lattices).

A large number of configurations are required to reach the statistical accuracy – $\mathcal{O}(5\%)$ at $\tau T = 1/2$ – needed for scaling test near the critical point. We have generated about $1 \cdot 10^6$ configurations on our smaller lattices and up to $4 \cdot 10^5$ on the large lattices.

The algorithm used to generate the configurations uses a standard mixture of heat-bath and over-relation updates in a typical ratio of 1:4-1:6 to keep correlations between consecutive configurations small. Autocorrelation times in the transition region range from $\mathcal{O}(1)$ on the small lattices to about 40 on the largest lattices.

Numerical simulations have been performed on the BlueGene/L, BlueGene/P at the New York Center for Computational Science (NYCCS), using a code developed specifically for this work.

Critical behavior of $G_{\Theta\Theta}$ – simulation details

We have calculated the correlation function $G_{\Theta\Theta}(\tau, T)$ close to the deconfinement transition point of the SU(2) gauge theory. In our simulation we use lattices of size $N_\sigma^3 N_\tau$ with $N_\tau = 4$. This gives us information on the correlation function at two non-zero values of Euclidean time, *i.e.* at $\tau T = 1/4$ and at the midpoint $\tau T = 1/2$.

Most of our simulations have been performed at temperatures close to the phase transition where the correlation length becomes large. This required calculations on large spatial lattices in order to eliminate finite volume effects.

We used spatial lattice sizes with aspect ratios N_σ / N_τ varying from 8 ($32^3 \times 4$ lattices) up to values as large as 32 ($128^3 \times 4$ lattices).

A large number of configurations are required to reach the statistical accuracy – $\mathcal{O}(5\%)$ at $\tau T = 1/2$ – needed for scaling test near the critical point. We have generated about $1 \cdot 10^6$ configurations on our smaller lattices and up to $4 \cdot 10^5$ on the large lattices.

The algorithm used to generate the configurations uses a standard mixture of heat-bath and over-relation updates in a typical ratio of 1:4-1:6 to keep correlations between consecutive configurations small. Autocorrelation times in the transition region range from $\mathcal{O}(1)$ on the small lattices to about 40 on the largest lattices.

Numerical simulations have been performed on the BlueGene/L, BlueGene/P at the New York Center for Computational Science (NYCCS), using a code developed specifically for this work.

Critical behavior of $G_{\Theta\Theta}$ – simulation details

We have calculated the correlation function $G_{\Theta\Theta}(\tau, T)$ close to the deconfinement transition point of the SU(2) gauge theory. In our simulation we use lattices of size $N_\sigma^3 N_\tau$ with $N_\tau = 4$. This gives us information on the correlation function at two non-zero values of Euclidean time, *i.e.* at $\tau T = 1/4$ and at the midpoint $\tau T = 1/2$.

Most of our simulations have been performed at temperatures close to the phase transition where the correlation length becomes large. This required calculations on large spatial lattices in order to eliminate finite volume effects.

We used spatial lattice sizes with aspect ratios N_σ / N_τ varying from 8 ($32^3 \times 4$ lattices) up to values as large as 32 ($128^3 \times 4$ lattices).

A large number of configurations are required to reach the statistical accuracy – $\mathcal{O}(5\%)$ at $\tau T = 1/2$ – needed for scaling test near the critical point. We have generated about $1 \cdot 10^6$ configurations on our smaller lattices and up to $4 \cdot 10^5$ on the large lattices.

The algorithm used to generate the configurations uses a standard mixture of heat-bath and over-relation updates in a typical ratio of 1:4-1:6 to keep correlations between consecutive configurations small. Autocorrelation times in the transition region range from $\mathcal{O}(1)$ on the small lattices to about 40 on the largest lattices.

Numerical simulations have been performed on the BlueGene/L, BlueGene/P at the New York Center for Computational Science (NYCCS), using a code developed specifically for this work.

Critical behavior of $G_{\Theta\Theta}$

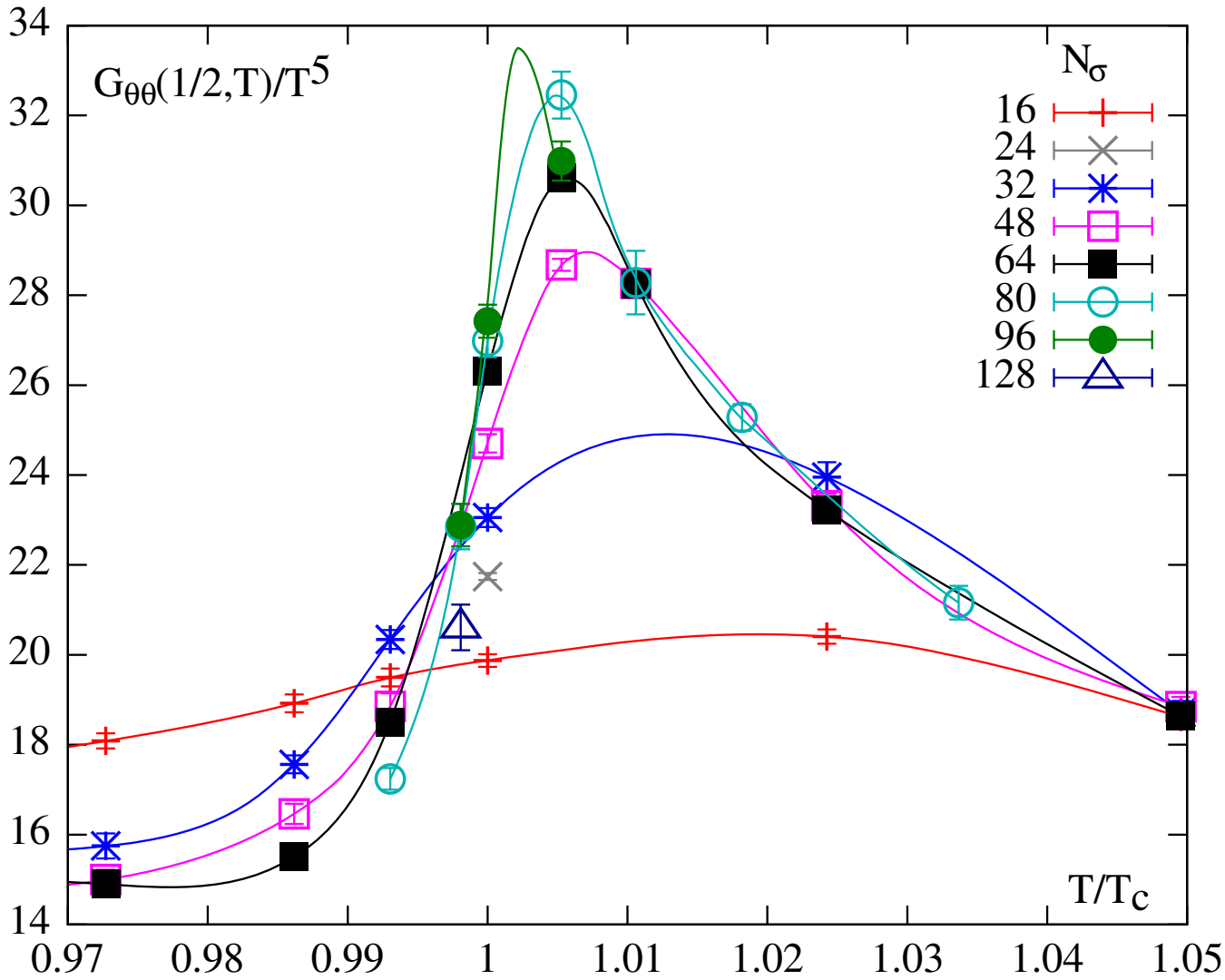

Critical behavior of $G_{\Theta\Theta}$ – finite size scaling at T_c

At T_c the singular part behavior of $G_{\Theta\Theta}$ is expected to be:

$$G_{\Theta\Theta}(\tau, T_c)/T_c^5 = A_\sigma N_\sigma^{\alpha/\nu}\left(1 + B_\sigma N_\sigma^{-\omega/\nu}\right) + C_\sigma \ ,$$

where A_σ, B_σ, C_σ might depend on Euclidean time.
This functional form gives excellent fits for both datasets at distance $\tau T = 1/4$ and $\tau T = 1/2$.

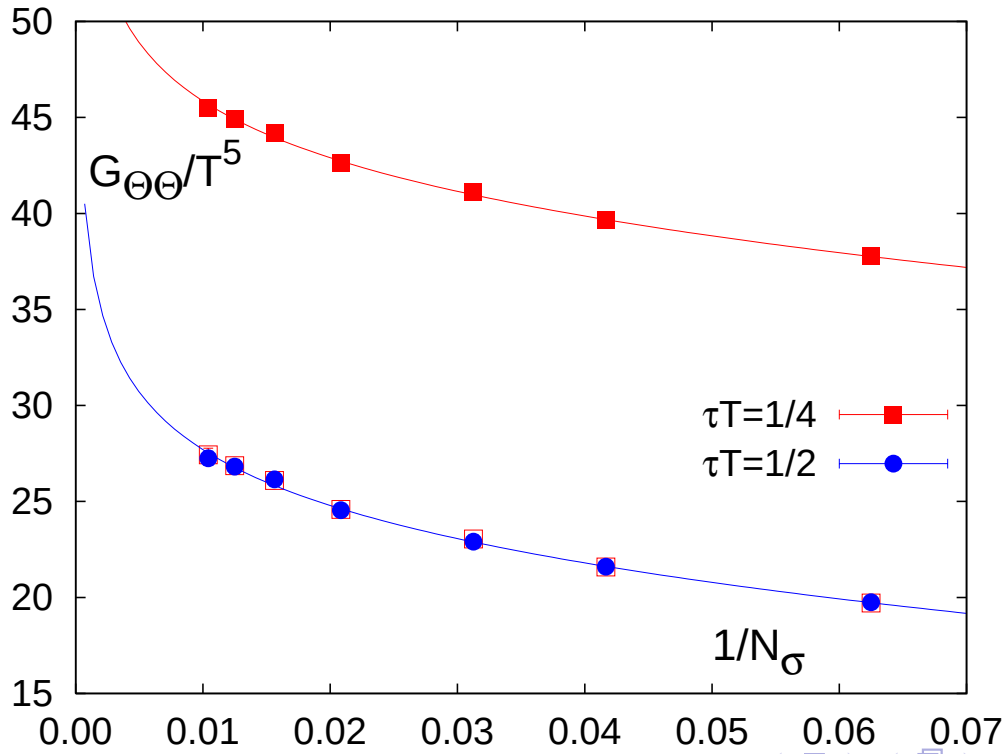

Critical behavior of $G_{\Theta\Theta}$ – finite size scaling at T_c

At T_c the singular part behavior of $G_{\Theta\Theta}$ is expected to be:

$$G_{\Theta\Theta}(\tau, T_c)/T_c^5 = A_\sigma N_\sigma^{\alpha/\nu}\left(1 + B_\sigma N_\sigma^{-\omega/\nu}\right) + C_\sigma \ ,$$

where A_σ, B_σ, C_σ might depend on Euclidean time.
This functional form gives excellent fits for both datasets at distance $\tau T = 1/4$ and $\tau T = 1/2$.

The fits yields:

$$\begin{aligned} A_\sigma(\tau T = 1/2)/A_\sigma(\tau T = 1/4) &= 1.01 \pm 0.19 \\ B_\sigma(\tau T = 1/2)/B_\sigma(\tau T = 1/4) &= 1.01 \pm 0.58 \ . \end{aligned}$$

This indicates that at T_c the singular contributions to $G_{\Theta\Theta}(\tau, T)$ are independent on the Euclidean time separation τ.

	τT	A_σ	B_σ	C_σ
free	1/4	9.2(1.2)	-2.4(1.0)	26.3(2.7)
fit	1/2	9.1(1.2)	-2.4(0.9)	8.4(2.9)
combined	1/4	9.15(73)	-2.39(59)	26.4(1.9)
fit	1/2			8.3(1.7)

Critical behavior of $G_{\Theta\Theta}$ – scaling in the critical region

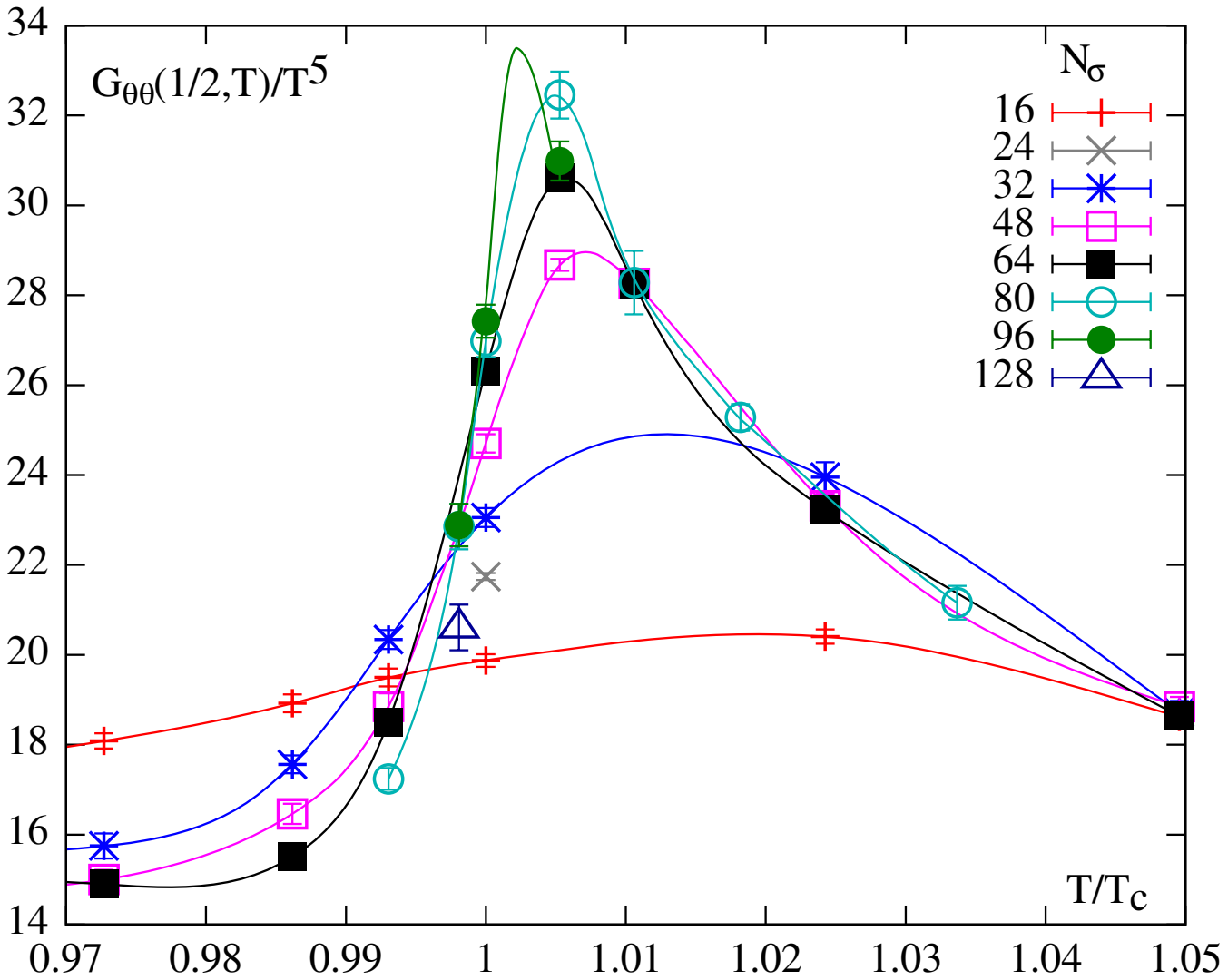

Critical behavior of $G_{\Theta\Theta}$ – scaling in the critical region

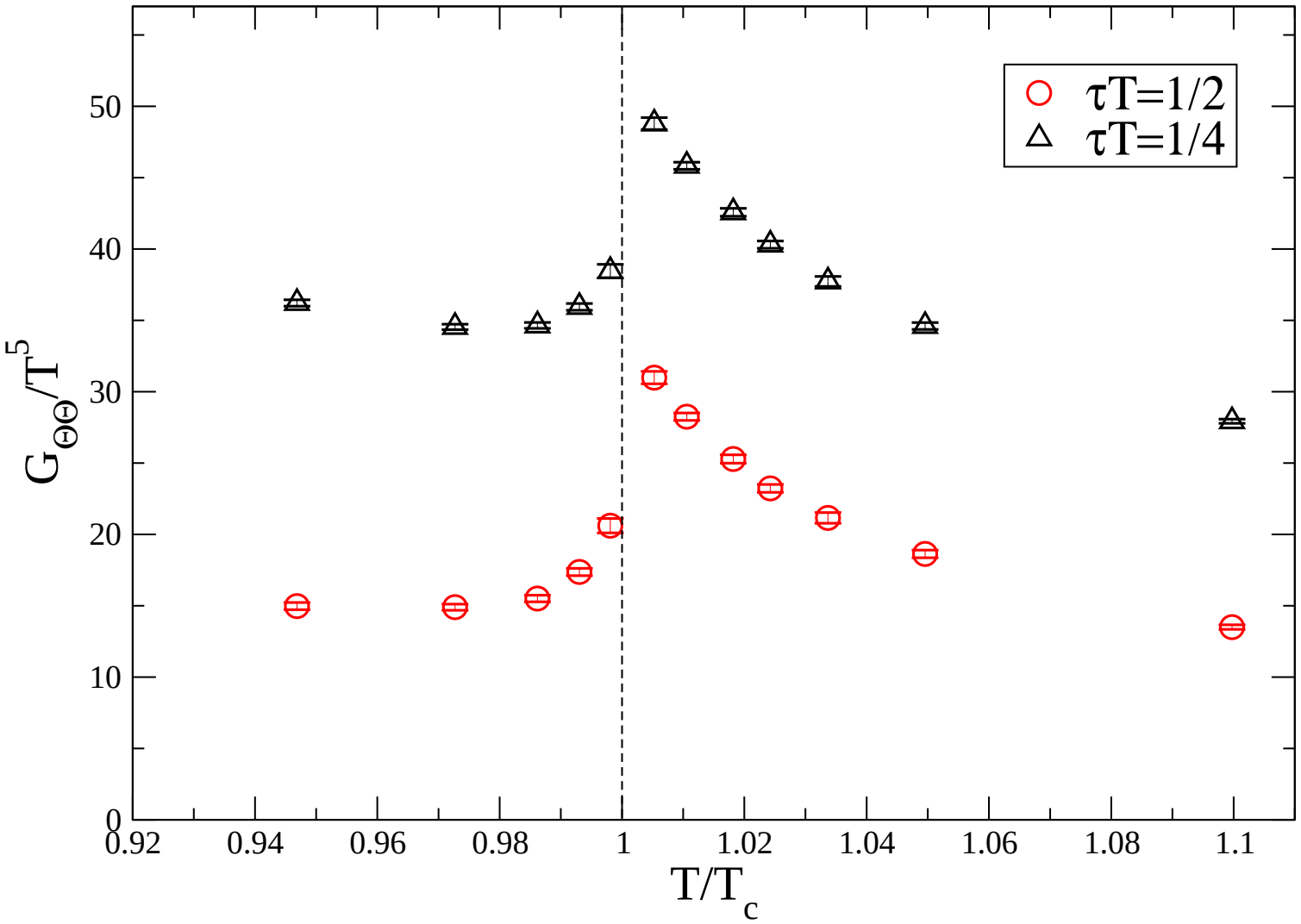

Critical behavior of $G_{\Theta\Theta}$ – scaling in the critical region

In the vicinity of T_c we expect the data to be well described by the scaling ansatz,

$$G_{\Theta\Theta}(\hat{\tau}, T)/T^5 = A_{\pm} t^{-\alpha}(1 + B_{\pm} t^{\omega}) + C + D\, t\ ,$$

where A_+, $B_\pm$, C, D are free parameters, which again all may depend on Euclidean time. This provides very good fits in the interval $T/T_c \in [0.94, 1.05]$.

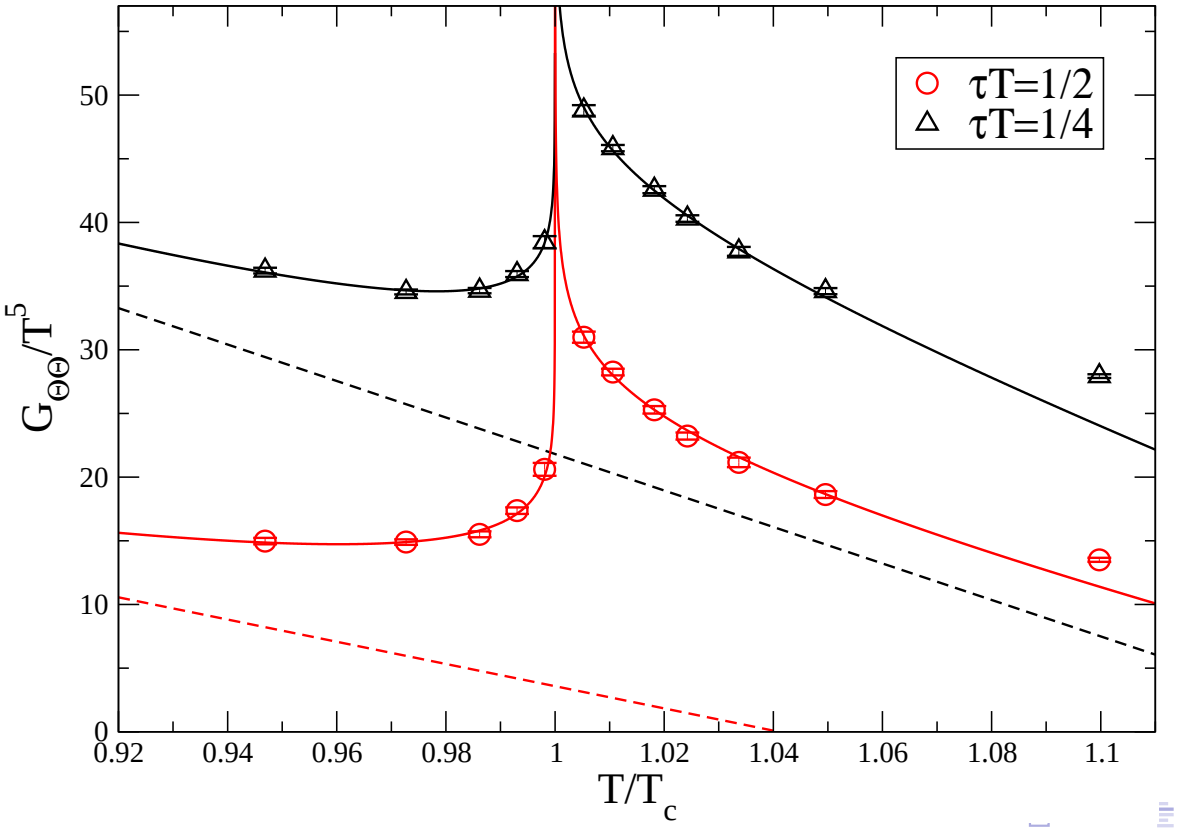

Critical behavior of $G_{\Theta\Theta}$ – scaling in the critical region

In the vicinity of T_c we expect the data to be well described by the scaling ansatz,

$$G_{\Theta\Theta}(\hat{\tau}, T)/T^5 = A_{\pm} t^{-\alpha}(1 + B_{\pm} t^{\omega}) + C + D\, t\ ,$$

where A_+, $B_\pm$, C, D are free parameters, which again all may depend on Euclidean time. This provides very good fits in the interval $T/T_c \in [0.94, 1.05]$.

Again we find that within errors the fit parameters A_+ and $B_\pm$ are independent of τ; a combined fit of $G_{\Theta\Theta}(1/4, T)/T^5$ and $G_{\Theta\Theta}(1/2, T)/T^5$ with common amplitudes A_+ and $B_\pm$ also gives a $\chi^2/dof = 1.1$.

	τT	A_+	B_+	B_-	C	D
free fit	1/4	16.3(2.1)	-0.59(19)	-1.9(1.4)	21.5(5.7)	-150(53)
	1/2	16.4(2.2)	-0.76(18)	-2.2(1.5)	3.7(3.4)	-95(32)
combined fit	1/4	16.5(1.3)	-0.74(10)	-2.12(86)	21.8(2.1)	-143(20)
	1/2				3.8(1.9)	-87(18)

Critical behavior of $G_{\Theta\Theta}$

The analysis presented establishes that the correlation function of the trace of the energy-momentum tensor shows the expected universal singular structure of the specific heat in a 3-dimensional Ising model. In the vicinity of T_c the singular contributions to $G_{\Theta\Theta}(\tau, T)$ are found to be independent of Euclidean time.

In order to eliminate the leading singular behavior from $G_{\Theta\Theta}$ it thus suffices to consider $\Delta G_{\Theta\Theta}(\tau, T) \equiv G_{\Theta\Theta}(\tau, T) - G_{\Theta\Theta}(1/2T, T)$.

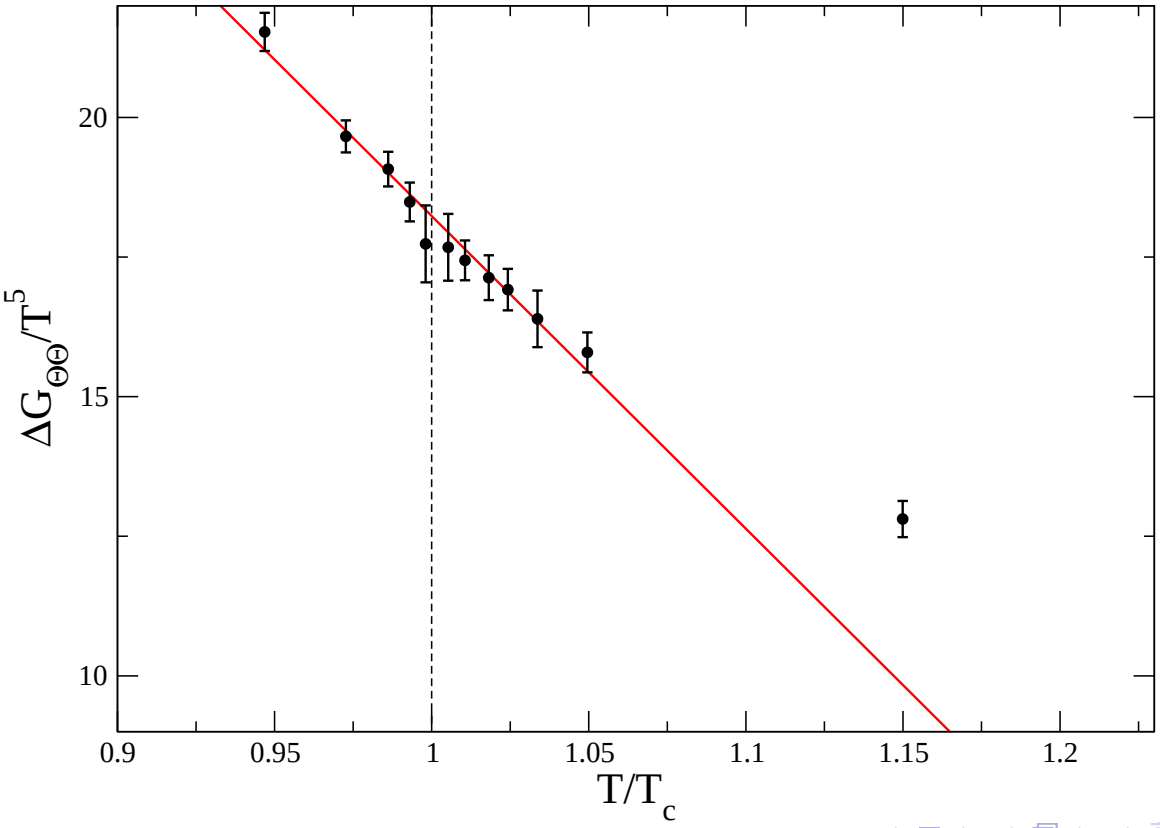

Critical behavior of $G_{\Theta\Theta}$

The analysis presented establishes that the correlation function of the trace of the energy-momentum tensor shows the expected universal singular structure of the specific heat in a 3-dimensional Ising model. In the vicinity of T_c the singular contributions to $G_{\Theta\Theta}(\tau, T)$ are found to be independent of Euclidean time.

In order to eliminate the leading singular behavior from $G_{\Theta\Theta}$ it thus suffices to consider $\Delta G_{\Theta\Theta}(\tau, T) \equiv G_{\Theta\Theta}(\tau, T) - G_{\Theta\Theta}(1/2T, T)$.

We have therefore explicitly shown that the singular term in $G_{\Theta\Theta}$ gives a contribution to its spectral function which is proportional to a delta function at zero frequency.

$$\rho_{\Theta\Theta}(\omega, T) = 9\rho_{pp}(\omega, T) + T\partial_T(\epsilon - 6p)\omega\delta(\omega) \ .$$

Correlation functions of $G_{\epsilon\epsilon}, G_{\epsilon p}, G_{pp}$

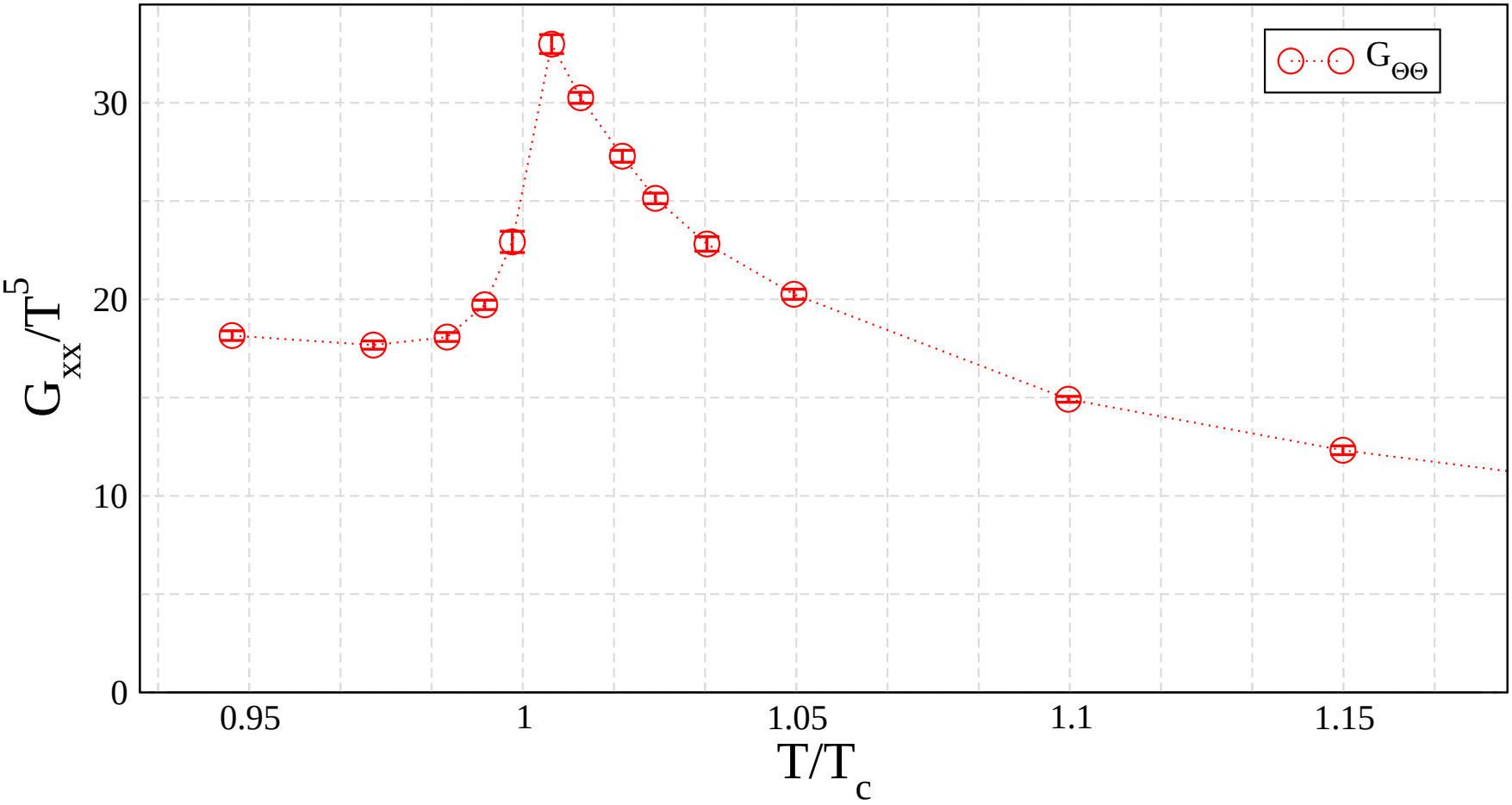

Correlation functions of $G_{\epsilon\epsilon}, G_{\epsilon p}, G_{pp}$

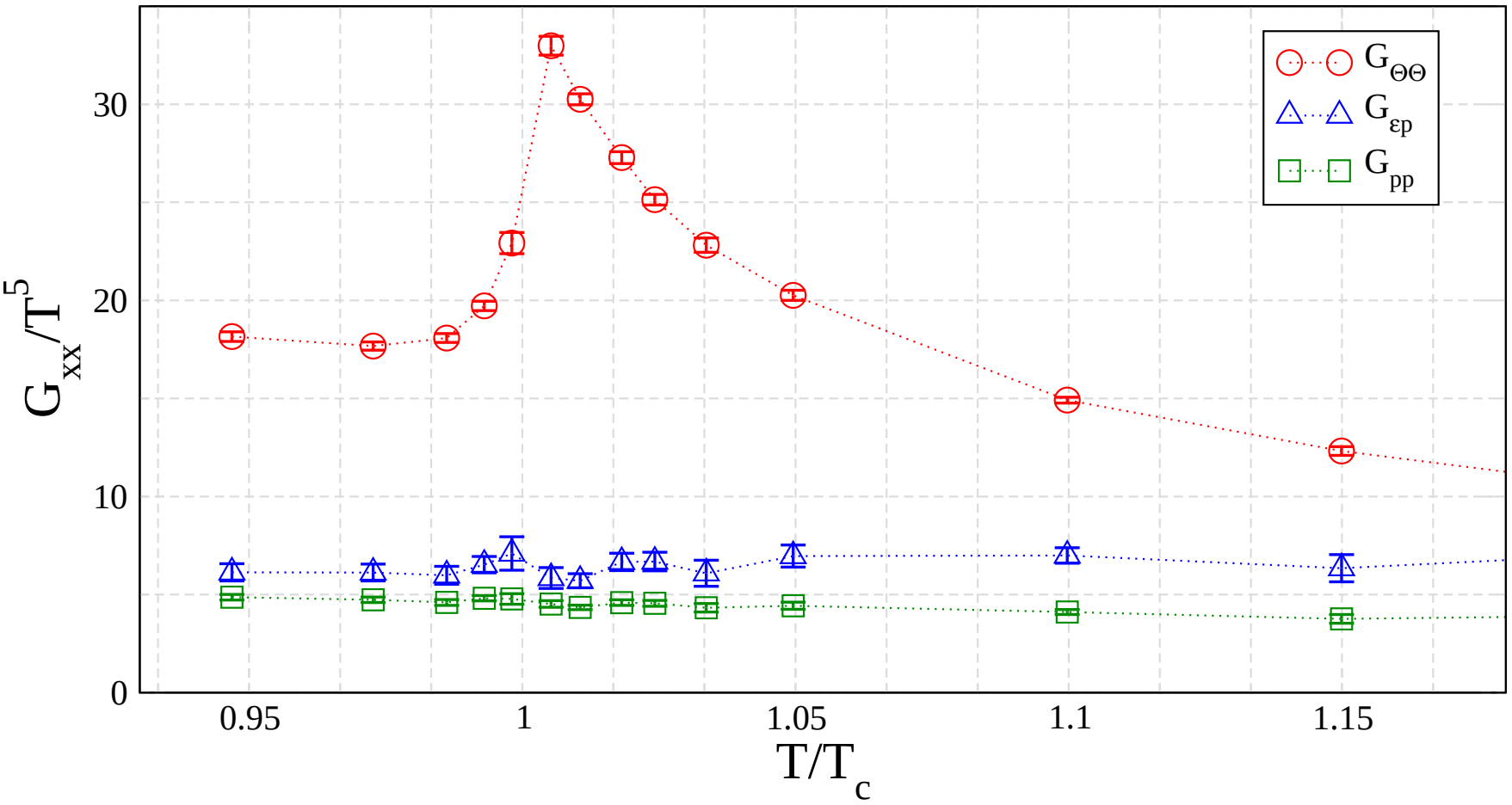

Correlation functions of $G_{\epsilon\epsilon}, G_{\epsilon p}, G_{pp}$

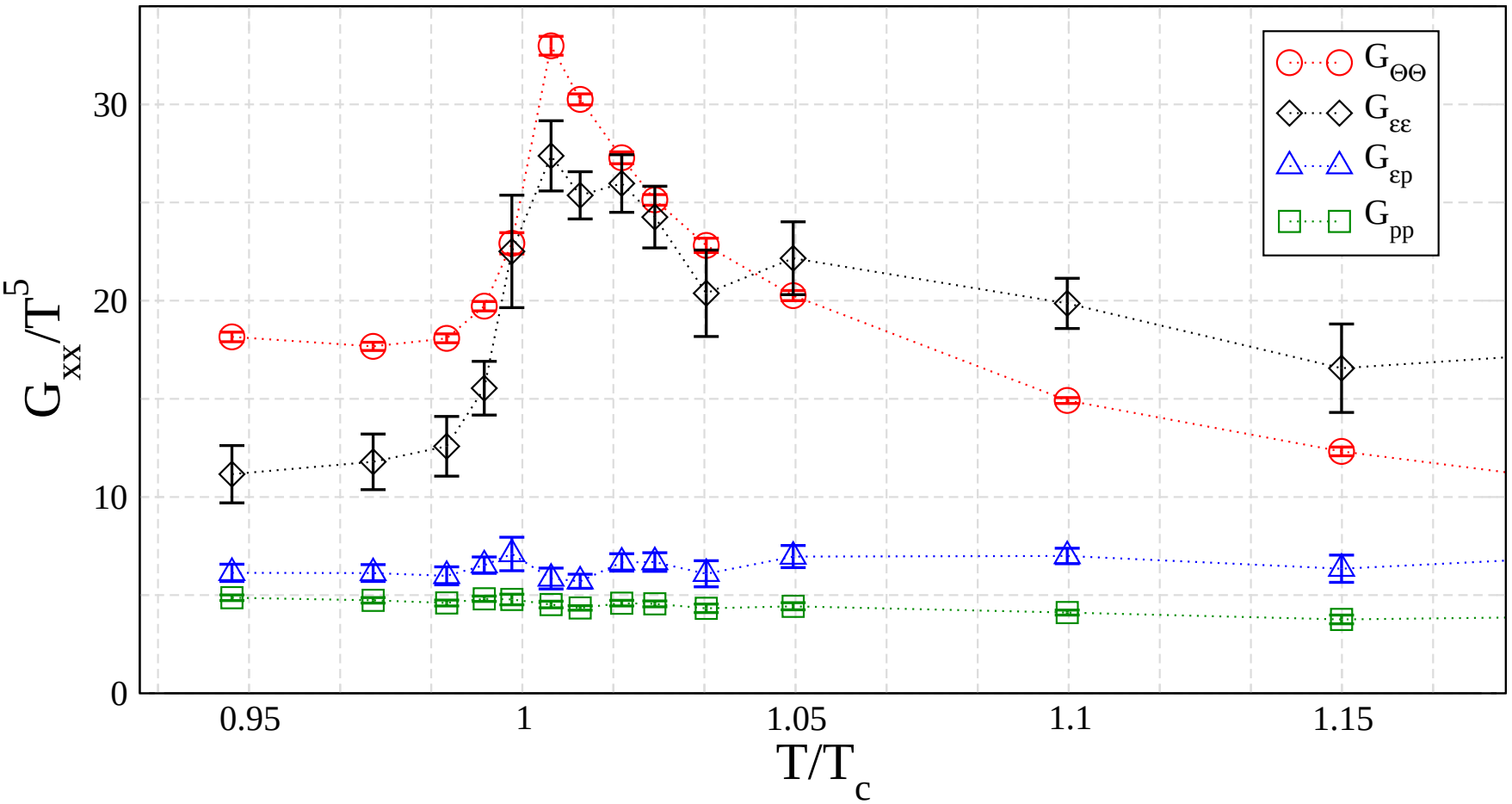

Considerations for the bulk viscosity

The pressure-pressure correlation function G_{pp} does not present any singular behavior. From this observation we cannot conclude however that the bulk viscosity itself is not diverging.

In fact consider a simple ansatz for the form of the spectral function ρ_{pp}:

$$\rho_{pp}(\omega, T) \equiv f(\omega, \zeta, \omega_0) + \rho_{>}(\omega, T) \ ,$$

where the low-frequency part is modeled by a Breit-Wigner:

$$f(\omega, \zeta, \omega_0) = \frac{1}{\pi} \zeta \frac{\omega \omega_0^2}{\omega^2 + \omega_0^2} \quad ,$$

with ζ and ω_0 both dependent on T. If approaching T_c, $\omega_0 \to 0$ we have:

$$G_{pp}(\tau, T) \propto T\zeta(T)\omega_0(T) + \mathcal{O}(\omega_0^2) + \text{high frequency part} \ .$$

We have therefore that the product $\zeta(T)\omega_0(T)$ remains finite at the critical temperature, while the bulk viscosity itself may or may not diverge.

The parameter ω_0 represent the characteristic frequency range over which ρ/ω remains constant and equal to ζ. Assuming that ω_0 is related to the inverse relaxation time we have: $\omega_0(t) \propto t^{z\nu}$, where z is a dynamical critical exponent $z \sim 2 - 3$.

This in turn implies that it is still possible that the bulk viscosity is rather strongly divergent at T_c while no visible singularity is visible in the pressure-pressure correlator.

Considerations for the bulk viscosity

The pressure-pressure correlation function G_{pp} does not present any singular behavior. From this observation we cannot conclude however that the bulk viscosity itself is not diverging.

In fact consider a simple ansatz for the form of the spectral function ρ_{pp}:

$$\rho_{pp}(\omega, T) \equiv f(\omega, \zeta, \omega_0) + \rho_{>}(\omega, T) \ ,$$

where the low-frequency part is modeled by a Breit-Wigner:

$$f(\omega, \zeta, \omega_0) = \frac{1}{\pi} \zeta \frac{\omega \omega_0^2}{\omega^2 + \omega_0^2} \quad ,$$

with ζ and ω_0 both dependent on T. If approaching T_c, $\omega_0 \to 0$ we have:

$$G_{pp}(\tau, T) \propto T\zeta(T)\omega_0(T) + \mathcal{O}(\omega_0^2) + \text{high frequency part} \ .$$

We have therefore that the product $\zeta(T)\omega_0(T)$ remains finite at the critical temperature, while the bulk viscosity itself may or may not diverge.

The parameter ω_0 represent the characteristic frequency range over which ρ/ω remains constant and equal to ζ. Assuming that ω_0 is related to the inverse relaxation time we have: $\omega_0(t) \propto t^{z\nu}$, where z is a dynamical critical exponent $z \sim 2 - 3$.

This in turn implies that it is still possible that the bulk viscosity is rather strongly divergent at T_c while no visible singularity is visible in the pressure-pressure correlator.

Considerations for the bulk viscosity

The pressure-pressure correlation function G_{pp} does not present any singular behavior. From this observation we cannot conclude however that the bulk viscosity itself is not diverging.

In fact consider a simple ansatz for the form of the spectral function ρ_{pp}:

$$\rho_{pp}(\omega, T) \equiv f(\omega, \zeta, \omega_0) + \rho_{>}(\omega, T) \ ,$$

where the low-frequency part is modeled by a Breit-Wigner:

$$f(\omega, \zeta, \omega_0) = \frac{1}{\pi} \zeta \frac{\omega \omega_0^2}{\omega^2 + \omega_0^2} \quad ,$$

with ζ and ω_0 both dependent on T. If approaching T_c, $\omega_0 \to 0$ we have:

$$G_{pp}(\tau, T) \propto T\zeta(T)\omega_0(T) + \mathcal{O}(\omega_0^2) + \text{high frequency part} \ .$$

We have therefore that the product $\zeta(T)\omega_0(T)$ remains finite at the critical temperature, while the bulk viscosity itself may or may not diverge.

The parameter ω_0 represent the characteristic frequency range over which ρ/ω remains constant and equal to ζ. Assuming that ω_0 is related to the inverse relaxation time we have: $\omega_0(t) \propto t^{z\nu}$, where z is a dynamical critical exponent $z \sim 2 - 3$.

This in turn implies that it is still possible that the bulk viscosity is rather strongly divergent at T_c while no visible singularity is visible in the pressure-pressure correlator.

Considerations for the bulk viscosity

The pressure-pressure correlation function G_{pp} does not present any singular behavior. From this observation we cannot conclude however that the bulk viscosity itself is not diverging.

In fact consider a simple ansatz for the form of the spectral function ρ_{pp}:

$$\rho_{pp}(\omega, T) \equiv f(\omega, \zeta, \omega_0) + \rho_{>}(\omega, T) \ ,$$

where the low-frequency part is modeled by a Breit-Wigner:

$$f(\omega, \zeta, \omega_0) = \frac{1}{\pi} \zeta \frac{\omega \omega_0^2}{\omega^2 + \omega_0^2} \quad ,$$

with ζ and ω_0 both dependent on T. If approaching T_c, $\omega_0 \to 0$ we have:

$$G_{pp}(\tau, T) \propto T\zeta(T)\omega_0(T) + \mathcal{O}(\omega_0^2) + \text{high frequency part} \ .$$

We have therefore that the product $\zeta(T)\omega_0(T)$ remains finite at the critical temperature, while the bulk viscosity itself may or may not diverge.

The parameter ω_0 represent the characteristic frequency range over which ρ/ω remains constant and equal to ζ. Assuming that ω_0 is related to the inverse relaxation time we have: $\omega_0(t) \propto t^{z\nu}$, where z is a dynamical critical exponent $z \sim 2 - 3$.

This in turn implies that it is still possible that the bulk viscosity is rather strongly divergent at T_c while no visible singularity is visible in the pressure-pressure correlator.

Outline

1 Introduction

2 SU(2) thermodynamics

3 Correlation functions

4 Conclusions

Conclusions

1. As a preliminary step, we have studied the thermodynamic properties of the SU(2) LGT at the deconfinement transition. Specifically the critical behavior of the pressure, energy density was analyzed and found in excellent agreement with the expected 3-d Ising critical behavior.
2. We have shown that the correlation function of the trace of the energy-momentum tensor $G_{\Theta\Theta}$ diverges at the critical temperature.
3. Using the finite size scaling at the critical temperature and the temperature scaling in the critical region, the singular structure of $G_{\Theta\Theta}$ was found to be consistent, with high accuracy, with that of the specific heat c_V.
4. We have shown that $G_{\Theta\Theta}$ becomes independent of Euclidean time at the critical point, which indicates that its spectral representation has a δ-function singularity at zero frequency.
5. The correlators $G_{\epsilon\epsilon}$, $G_{\epsilon p}$ and G_{pp} were also analyzed. The singular behavior of $G_{\Theta\Theta}$ can be traced back in the corresponding singular behavior of $G_{\epsilon\epsilon}$, while the other two correlation functions remain finite at the critical point.

Thank You!

Conclusions

1. As a preliminary step, we have studied the thermodynamic properties of the SU(2) LGT at the deconfinement transition. Specifically the critical behavior of the pressure, energy density was analyzed and found in excellent agreement with the expected 3-d Ising critical behavior.
2. We have shown that the correlation function of the trace of the energy-momentum tensor $G_{\Theta\Theta}$ diverges at the critical temperature.
3. Using the finite size scaling at the critical temperature and the temperature scaling in the critical region, the singular structure of $G_{\Theta\Theta}$ was found to be consistent, with high accuracy, with that of the specific heat c_V.
4. We have shown that $G_{\Theta\Theta}$ becomes independent of Euclidean time at the critical point, which indicates that its spectral representation has a δ-function singularity at zero frequency.
5. The correlators $G_{\epsilon\epsilon}$, $G_{\epsilon p}$ and G_{pp} were also analyzed. The singular behavior of $G_{\Theta\Theta}$ can be traced back in the corresponding singular behavior of $G_{\epsilon\epsilon}$, while the other two correlation functions remain finite at the critical point.

Thank You!

Conclusions

1. As a preliminary step, we have studied the thermodynamic properties of the SU(2) LGT at the deconfinement transition. Specifically the critical behavior of the pressure, energy density was analyzed and found in excellent agreement with the expected 3-d Ising critical behavior.
2. We have shown that the correlation function of the trace of the energy-momentum tensor $G_{\Theta\Theta}$ diverges at the critical temperature.
3. Using the finite size scaling at the critical temperature and the temperature scaling in the critical region, the singular structure of $G_{\Theta\Theta}$ was found to be consistent, with high accuracy, with that of the specific heat c_V.
4. We have shown that $G_{\Theta\Theta}$ becomes independent of Euclidean time at the critical point, which indicates that its spectral representation has a δ-function singularity at zero frequency.
5. The correlators $G_{\epsilon\epsilon}$, $G_{\epsilon p}$ and G_{pp} were also analyzed. The singular behavior of $G_{\Theta\Theta}$ can be traced back in the corresponding singular behavior of $G_{\epsilon\epsilon}$, while the other two correlation functions remain finite at the critical point.

Thank You!

Conclusions

1. As a preliminary step, we have studied the thermodynamic properties of the SU(2) LGT at the deconfinement transition. Specifically the critical behavior of the pressure, energy density was analyzed and found in excellent agreement with the expected 3-d Ising critical behavior.
2. We have shown that the correlation function of the trace of the energy-momentum tensor $G_{\Theta\Theta}$ diverges at the critical temperature.
3. Using the finite size scaling at the critical temperature and the temperature scaling in the critical region, the singular structure of $G_{\Theta\Theta}$ was found to be consistent, with high accuracy, with that of the specific heat c_V.
4. We have shown that $G_{\Theta\Theta}$ becomes independent of Euclidean time at the critical point, which indicates that its spectral representation has a δ-function singularity at zero frequency.
5. The correlators $G_{\epsilon\epsilon}$, $G_{\epsilon p}$ and G_{pp} were also analyzed. The singular behavior of $G_{\Theta\Theta}$ can be traced back in the corresponding singular behavior of $G_{\epsilon\epsilon}$, while the other two correlation functions remain finite at the critical point.

Thank You!

Conclusions

1. As a preliminary step, we have studied the thermodynamic properties of the SU(2) LGT at the deconfinement transition. Specifically the critical behavior of the pressure, energy density was analyzed and found in excellent agreement with the expected 3-d Ising critical behavior.
2. We have shown that the correlation function of the trace of the energy-momentum tensor $G_{\Theta\Theta}$ diverges at the critical temperature.
3. Using the finite size scaling at the critical temperature and the temperature scaling in the critical region, the singular structure of $G_{\Theta\Theta}$ was found to be consistent, with high accuracy, with that of the specific heat c_V.
4. We have shown that $G_{\Theta\Theta}$ becomes independent of Euclidean time at the critical point, which indicates that its spectral representation has a δ-function singularity at zero frequency.
5. The correlators $G_{\epsilon\epsilon}$, $G_{\epsilon p}$ and G_{pp} were also analyzed. The singular behavior of $G_{\Theta\Theta}$ can be traced back in the corresponding singular behavior of $G_{\epsilon\epsilon}$, while the other two correlation functions remain finite at the critical point.

Thank You!

Conclusions

1. As a preliminary step, we have studied the thermodynamic properties of the SU(2) LGT at the deconfinement transition. Specifically the critical behavior of the pressure, energy density was analyzed and found in excellent agreement with the expected 3-d Ising critical behavior.
2. We have shown that the correlation function of the trace of the energy-momentum tensor $G_{\Theta\Theta}$ diverges at the critical temperature.
3. Using the finite size scaling at the critical temperature and the temperature scaling in the critical region, the singular structure of $G_{\Theta\Theta}$ was found to be consistent, with high accuracy, with that of the specific heat c_V.
4. We have shown that $G_{\Theta\Theta}$ becomes independent of Euclidean time at the critical point, which indicates that its spectral representation has a δ-function singularity at zero frequency.
5. The correlators $G_{\epsilon\epsilon}$, $G_{\epsilon p}$ and G_{pp} were also analyzed. The singular behavior of $G_{\Theta\Theta}$ can be traced back in the corresponding singular behavior of $G_{\epsilon\epsilon}$, while the other two correlation functions remain finite at the critical point.

Thank You!

Conclusions

1. As a preliminary step, we have studied the thermodynamic properties of the SU(2) LGT at the deconfinement transition. Specifically the critical behavior of the pressure, energy density was analyzed and found in excellent agreement with the expected 3-d Ising critical behavior.
2. We have shown that the correlation function of the trace of the energy-momentum tensor $G_{\Theta\Theta}$ diverges at the critical temperature.
3. Using the finite size scaling at the critical temperature and the temperature scaling in the critical region, the singular structure of $G_{\Theta\Theta}$ was found to be consistent, with high accuracy, with that of the specific heat c_V.
4. We have shown that $G_{\Theta\Theta}$ becomes independent of Euclidean time at the critical point, which indicates that its spectral representation has a δ-function singularity at zero frequency.
5. The correlators $G_{\epsilon\epsilon}$, $G_{\epsilon p}$ and G_{pp} were also analyzed. The singular behavior of $G_{\Theta\Theta}$ can be traced back in the corresponding singular behavior of $G_{\epsilon\epsilon}$, while the other two correlation functions remain finite at the critical point.

Thank You!

Backup Slides

Critical energy density and pressure

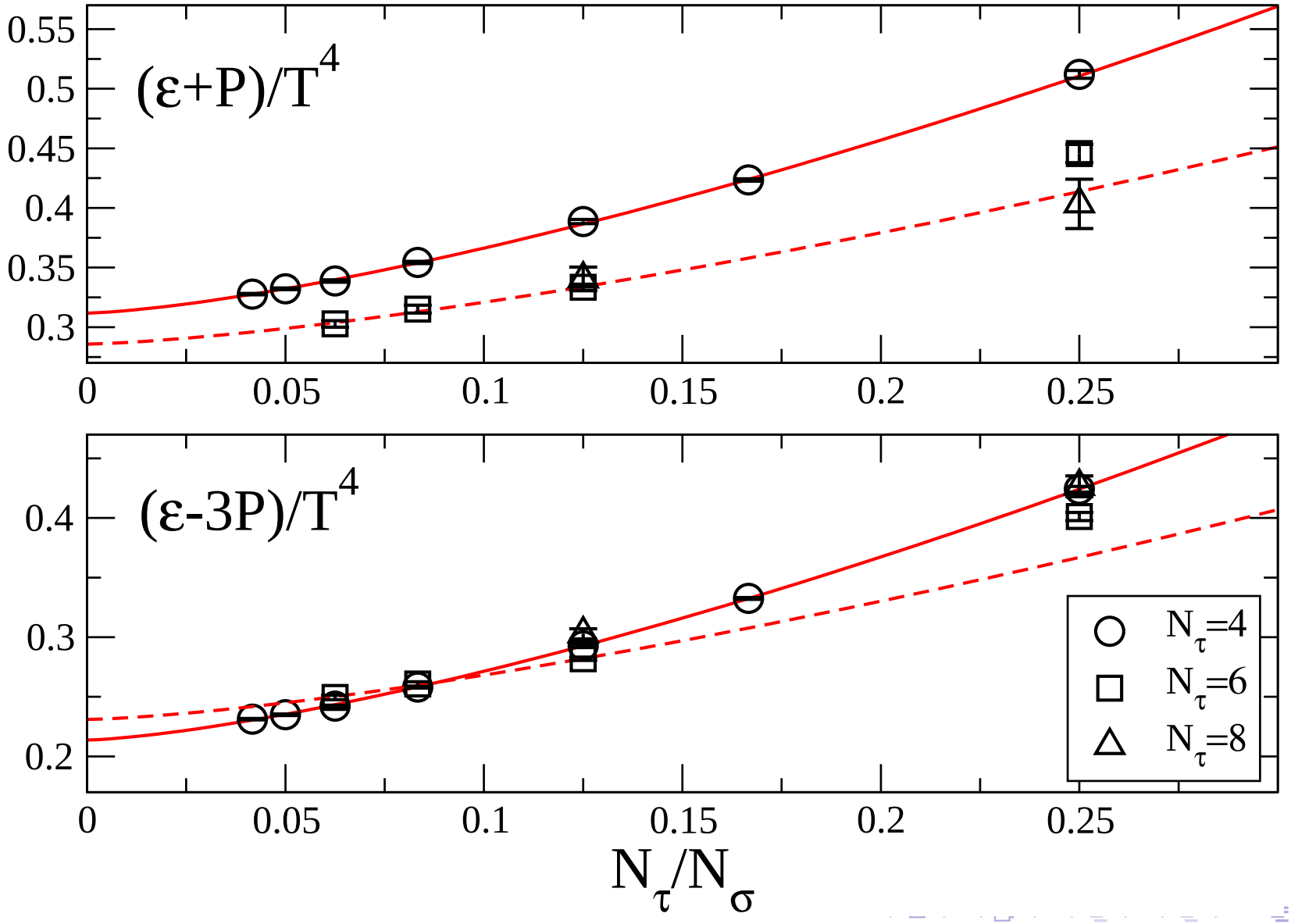

Definition of local operators

The differential formalism provides a straightforward way to introduce local lattice operators for the energy density and pressure.
For example:

$$\frac{\Theta^{\mu\mu}(\vec{x}, x_4)}{T^4} = 6NN_\tau^4 B(g^{-2}) \left(P_\sigma(\vec{x}, x_4) + P_\tau(\vec{x}, x_4) - 2P_0\right)$$

This is the simplest choice of a local expression for ϵ, p, $\Theta^{\mu\mu}$ and s and we will denote it in the following as *discretization scheme 1*.

We have also considered 2 other possibilities, denoted in the following as discretization scheme 2 and 3. They are defined by the following substitutions:

$$\text{scheme 2: } P_\sigma(x) \quad \rightarrow \quad \frac{1}{2}\left[P_\sigma(x) + P_\sigma(x + \hat{e}_4)\right]$$

$$\text{scheme 3: } P_\tau(x) \quad \rightarrow \quad \frac{1}{2}\left[P_\tau(x) + P_\tau(x - \hat{e}_4)\right]$$

All of the above schemes have $\mathcal{O}(a^2)$ discretization errors. Comparing different discretization schemes will allow to estimate these systematic effects.

Definition of local operators

The differential formalism provides a straightforward way to introduce local lattice operators for the energy density and pressure.
For example:

$$\frac{\Theta^{\mu\mu}(\vec{x}, x_4)}{T^4} = 6NN_\tau^4 B(g^{-2}) \left(P_\sigma(\vec{x}, x_4) + P_\tau(\vec{x}, x_4) - 2P_0\right)$$

This is the simplest choice of a local expression for ϵ, p, $\Theta^{\mu\mu}$ and s and we will denote it in the following as *discretization scheme 1*.

We have also considered 2 other possibilities, denoted in the following as discretization scheme 2 and 3. They are defined by the following substitutions:

$$\text{scheme 2: } P_\sigma(x) \quad \rightarrow \quad \frac{1}{2}\left[P_\sigma(x) + P_\sigma(x + \hat{e}_4)\right]$$

$$\text{scheme 3: } P_\tau(x) \quad \rightarrow \quad \frac{1}{2}\left[P_\tau(x) + P_\tau(x - \hat{e}_4)\right]$$

All of the above schemes have $\mathcal{O}(a^2)$ discretization errors. Comparing different discretization schemes will allow to estimate these systematic effects.

Definition of local operators

The differential formalism provides a straightforward way to introduce local lattice operators for the energy density and pressure.
For example:

$$\frac{\Theta^{\mu\mu}(\vec{x}, x_4)}{T^4} = 6NN_\tau^4 B(g^{-2}) \left(P_\sigma(\vec{x}, x_4) + P_\tau(\vec{x}, x_4) - 2P_0\right)$$

This is the simplest choice of a local expression for ϵ, p, $\Theta^{\mu\mu}$ and s and we will denote it in the following as *discretization scheme 1*.

We have also considered 2 other possibilities, denoted in the following as discretization scheme 2 and 3. They are defined by the following substitutions:

$$\text{scheme 2: } P_\sigma(x) \quad \rightarrow \quad \frac{1}{2}\left[P_\sigma(x) + P_\sigma(x + \hat{e}_4)\right]$$

$$\text{scheme 3: } P_\tau(x) \quad \rightarrow \quad \frac{1}{2}\left[P_\tau(x) + P_\tau(x - \hat{e}_4)\right]$$

All of the above schemes have $\mathcal{O}(a^2)$ discretization errors. Comparing different discretization schemes will allow to estimate these systematic effects.

Definition of local operators

The differential formalism provides a straightforward way to introduce local lattice operators for the energy density and pressure.
For example:

$$\frac{\Theta^{\mu\mu}(\vec{x}, x_4)}{T^4} = 6NN_\tau^4 B(g^{-2}) \left(P_\sigma(\vec{x}, x_4) + P_\tau(\vec{x}, x_4) - 2P_0\right)$$

This is the simplest choice of a local expression for ϵ, p, $\Theta^{\mu\mu}$ and s and we will denote it in the following as *discretization scheme 1*.

We have also considered 2 other possibilities, denoted in the following as discretization scheme 2 and 3. They are defined by the following substitutions:

$$\text{scheme 2: } P_\sigma(x) \quad \rightarrow \quad \frac{1}{2}\left[P_\sigma(x) + P_\sigma(x + \hat{e}_4)\right]$$

$$\text{scheme 3: } P_\tau(x) \quad \rightarrow \quad \frac{1}{2}\left[P_\tau(x) + P_\tau(x - \hat{e}_4)\right]$$

All of the above schemes have $\mathcal{O}(a^2)$ discretization errors. Comparing different discretization schemes will allow to estimate these systematic effects.

Zero momentum correlation functions

In the following we will always consider zero-momentum correlation functions. We introduce zero-momentum projected operators and their fluctuations:

$$\begin{aligned} Y(\tau) &= \frac{1}{N_\sigma^3} \sum_{\vec{x}} Y(\vec{x},\tau) \, , \\ \bar{Y}(\tau) &= Y(\tau) - \langle Y(\tau) \rangle \, . \end{aligned}$$

Connected correlation functions are then obtained as thermal averages of products of fluctuation operator:

$$\frac{G_{XY}(\tau,T)}{T^5} = N_\tau^5 \langle \bar{X}(\tau) \bar{Y}(0) \rangle \, .$$

It will also be useful to consider the following difference of correlators:

$$\frac{\Delta G_{XY}(\tau,T)}{T^5} = N_\tau^5 \left[\langle X(\tau) Y(0) \rangle - \langle X(\frac{1}{2T}) Y(0) \rangle \right] \, .$$

Note that the constant P_0 entering in the expression of ϵ, p and $\Theta^{\mu\mu}$ can be neglected in the correlation functions G_{XY} and ΔG_{XY}.

Zero momentum correlation functions

In the following we will always consider zero-momentum correlation functions. We introduce zero-momentum projected operators and their fluctuations:

$$\begin{aligned} Y(\tau) &= \frac{1}{N_\sigma^3} \sum_{\vec{x}} Y(\vec{x},\tau) \ , \\ \bar{Y}(\tau) &= Y(\tau) - \langle Y(\tau) \rangle \ . \end{aligned}$$

Connected correlation functions are then obtained as thermal averages of products of fluctuation operator:

$$\frac{G_{XY}(\tau,T)}{T^5} = N_\tau^5 \langle \bar{X}(\tau) \bar{Y}(0) \rangle \ .$$

It will also be useful to consider the following difference of correlators:

$$\frac{\Delta G_{XY}(\tau,T)}{T^5} = N_\tau^5 \left[\langle X(\tau) Y(0) \rangle - \langle X(\frac{1}{2T}) Y(0) \rangle \right] \ .$$

Note that the constant P_0 entering in the expression of ϵ, p and $\Theta^{\mu\mu}$ can be neglected in the correlation functions G_{XY} and ΔG_{XY}.

Zero momentum correlation functions

In the following we will always consider zero-momentum correlation functions. We introduce zero-momentum projected operators and their fluctuations:

$$\begin{aligned} Y(\tau) &= \frac{1}{N_\sigma^3} \sum_{\vec{x}} Y(\vec{x},\tau) \ , \\ \bar{Y}(\tau) &= Y(\tau) - \langle Y(\tau) \rangle \ . \end{aligned}$$

Connected correlation functions are then obtained as thermal averages of products of fluctuation operator:

$$\frac{G_{XY}(\tau,T)}{T^5} = N_\tau^5 \langle \bar{X}(\tau) \bar{Y}(0) \rangle \ .$$

It will also be useful to consider the following difference of correlators:

$$\frac{\Delta G_{XY}(\tau,T)}{T^5} = N_\tau^5 \left[\langle X(\tau) Y(0) \rangle - \langle X(\frac{1}{2T}) Y(0) \rangle \right] \ .$$

Note that the constant P_0 entering in the expression of ϵ, p and $\Theta^{\mu\mu}$ can be neglected in the correlation functions G_{XY} and ΔG_{XY}.

Zero momentum correlation functions

In the following we will always consider zero-momentum correlation functions. We introduce zero-momentum projected operators and their fluctuations:

$$\begin{aligned} Y(\tau) &= \frac{1}{N_\sigma^3} \sum_{\vec{x}} Y(\vec{x},\tau) \ , \\ \bar{Y}(\tau) &= Y(\tau) - \langle Y(\tau) \rangle \ . \end{aligned}$$

Connected correlation functions are then obtained as thermal averages of products of fluctuation operator:

$$\frac{G_{XY}(\tau,T)}{T^5} = N_\tau^5 \langle \bar{X}(\tau) \bar{Y}(0) \rangle \ .$$

It will also be useful to consider the following difference of correlators:

$$\frac{\Delta G_{XY}(\tau,T)}{T^5} = N_\tau^5 \left[\langle X(\tau) Y(0) \rangle - \langle X(\frac{1}{2T}) Y(0) \rangle \right] \ .$$

Note that the constant P_0 entering in the expression of ϵ, p and $\Theta^{\mu\mu}$ can be neglected in the correlation functions G_{XY} and ΔG_{XY}.

Correlation functions of $G_{\epsilon\epsilon}, G_{\epsilon p}, G_{pp}$

Since

$$G_{\Theta\Theta}(\tau, T) = G_{\epsilon\epsilon}(\tau, T) - 6G_{\epsilon p}(\tau, T) + 9G_{pp}(\tau, T) \ ,$$

we have:

$$\Delta G_{\Theta\Theta}(\tau, T) = \Delta G_{\epsilon\epsilon}(\tau, T) - 6\Delta G_{\epsilon p}(\tau, T) + 9\Delta G_{pp}(\tau, T) \simeq 9\Delta G_{pp}(\tau, T) \ .$$

The last equality is expected in the continuum limit since the correlation functions involving the energy density operator $\Delta G_{\epsilon Y}$ vanish.

This relation would allow in principle to use the correlation function $\Delta G_{\Theta\Theta}$ – which seems to be much easier to determine numerically – instead of G_{pp} for the determination of the bulk viscosity, without having to worry about the delta function singularity in the spectral function of $G_{\Theta\Theta}$.

However the independence on the time separation τ of $G_{\epsilon\epsilon}$ and $G_{\epsilon p}$ is required. At finite lattice spacing violations of order $\mathcal{O}(a^2)$ are expected.

We found in fact that for our $N_\tau = 4$ lattices such cut-off effects are large.

Correlation functions of $G_{\epsilon\epsilon}, G_{\epsilon p}, G_{pp}$

Since

$$G_{\Theta\Theta}(\tau, T) = G_{\epsilon\epsilon}(\tau, T) - 6G_{\epsilon p}(\tau, T) + 9G_{pp}(\tau, T) \ ,$$

we have:

$$\Delta G_{\Theta\Theta}(\tau, T) = \Delta G_{\epsilon\epsilon}(\tau, T) - 6\Delta G_{\epsilon p}(\tau, T) + 9\Delta G_{pp}(\tau, T) \simeq 9\Delta G_{pp}(\tau, T) \ .$$

The last equality is expected in the continuum limit since the correlation functions involving the energy density operator $\Delta G_{\epsilon Y}$ vanish.

This relation would allow in principle to use the correlation function $\Delta G_{\Theta\Theta}$ – which seems to be much easier to determine numerically – instead of G_{pp} for the determination of the bulk viscosity, without having to worry about the delta function singularity in the spectral function of $G_{\Theta\Theta}$.

However the independence on the time separation τ of $G_{\epsilon\epsilon}$ and $G_{\epsilon p}$ is required. At finite lattice spacing violations of order $\mathcal{O}(a^2)$ are expected.

We found in fact that for our $N_\tau = 4$ lattices such cut-off effects are large.

Correlation functions of $G_{\epsilon\epsilon}, G_{\epsilon p}, G_{pp}$

Since

$$G_{\Theta\Theta}(\tau, T) = G_{\epsilon\epsilon}(\tau, T) - 6G_{\epsilon p}(\tau, T) + 9G_{pp}(\tau, T) \ ,$$

we have:

$$\Delta G_{\Theta\Theta}(\tau, T) = \Delta G_{\epsilon\epsilon}(\tau, T) - 6\Delta G_{\epsilon p}(\tau, T) + 9\Delta G_{pp}(\tau, T) \simeq 9\Delta G_{pp}(\tau, T) \ .$$

The last equality is expected in the continuum limit since the correlation functions involving the energy density operator $\Delta G_{\epsilon Y}$ vanish.

This relation would allow in principle to use the correlation function $\Delta G_{\Theta\Theta}$ – which seems to be much easier to determine numerically – instead of G_{pp} for the determination of the bulk viscosity, without having to worry about the delta function singularity in the spectral function of $G_{\Theta\Theta}$.

However the independence on the time separation τ of $G_{\epsilon\epsilon}$ and $G_{\epsilon p}$ is required. At finite lattice spacing violations of order $\mathcal{O}(a^2)$ are expected.

We found in fact that for our $N_\tau = 4$ lattices such cut-off effects are large.

Discretization errors

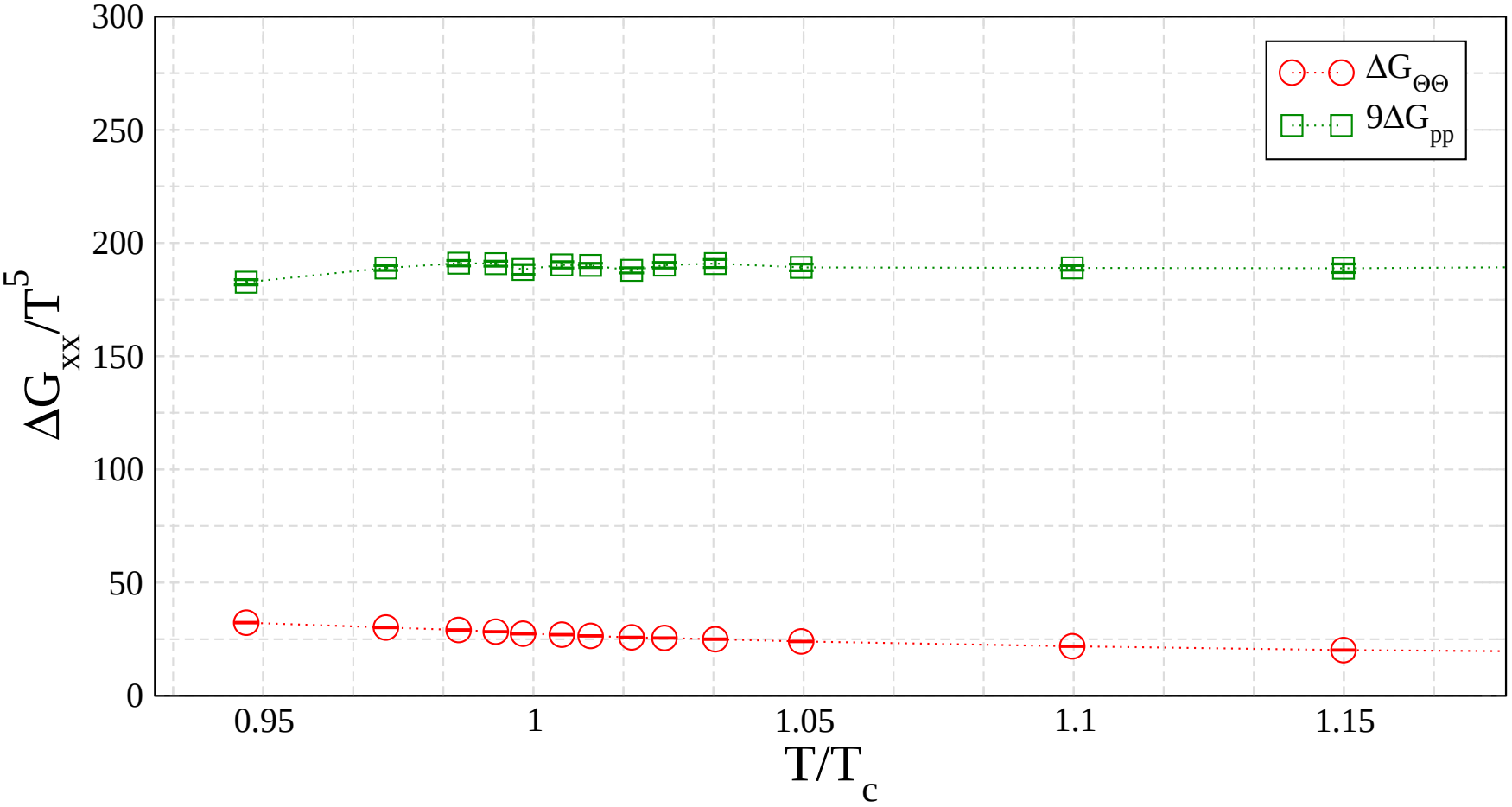

Discretization errors

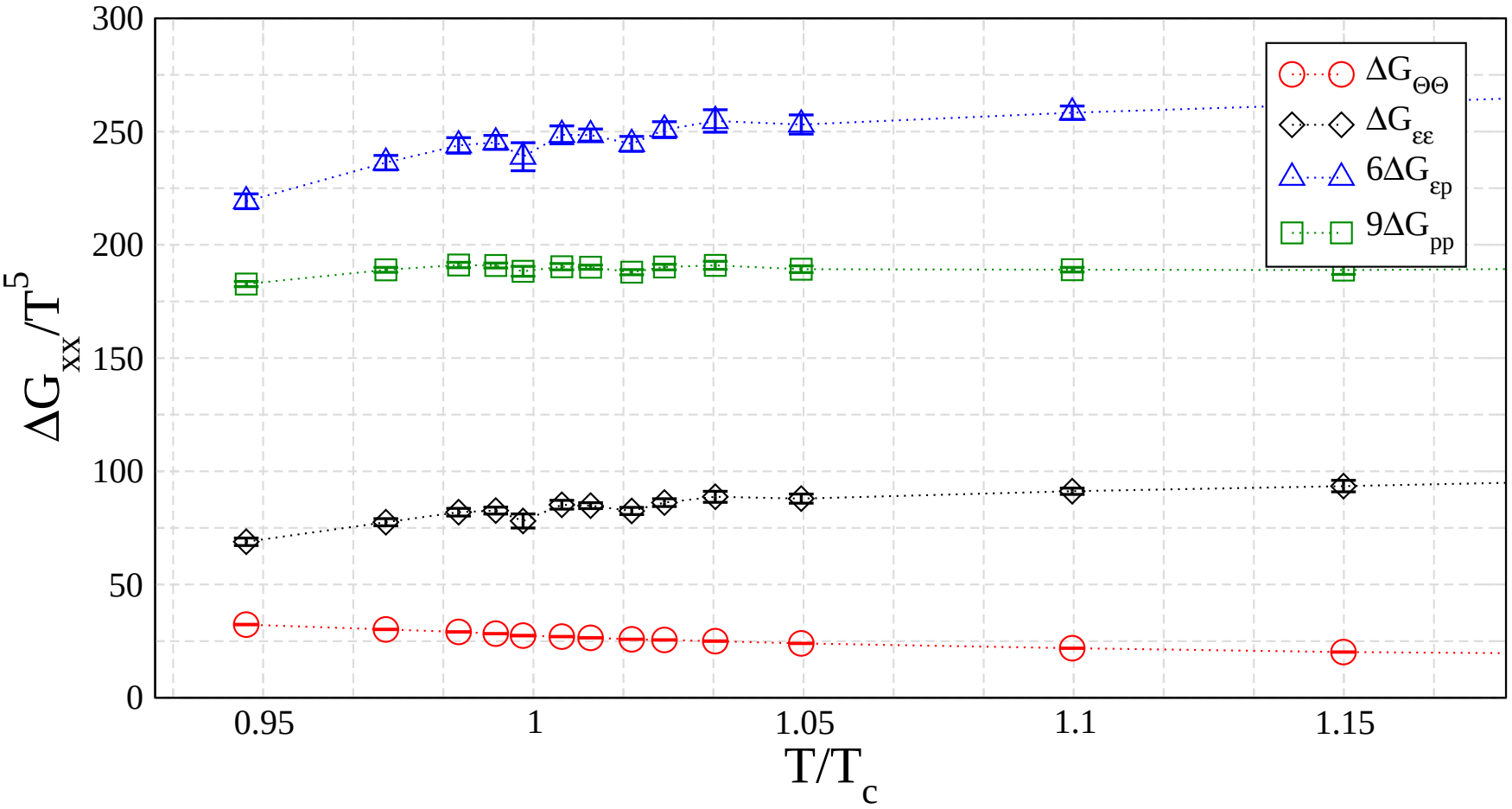

Discretization errors

It is clearly seen that for $N_\tau = 4$ lattices the correlation function $G_{\epsilon\epsilon}$ and $G_{\epsilon p}$ are not constant.

We can look at the magnitude of discretization effects in the correlators comparing different discretization schemes. Cut-off effects seems to be quite big for the correlation functions considered.

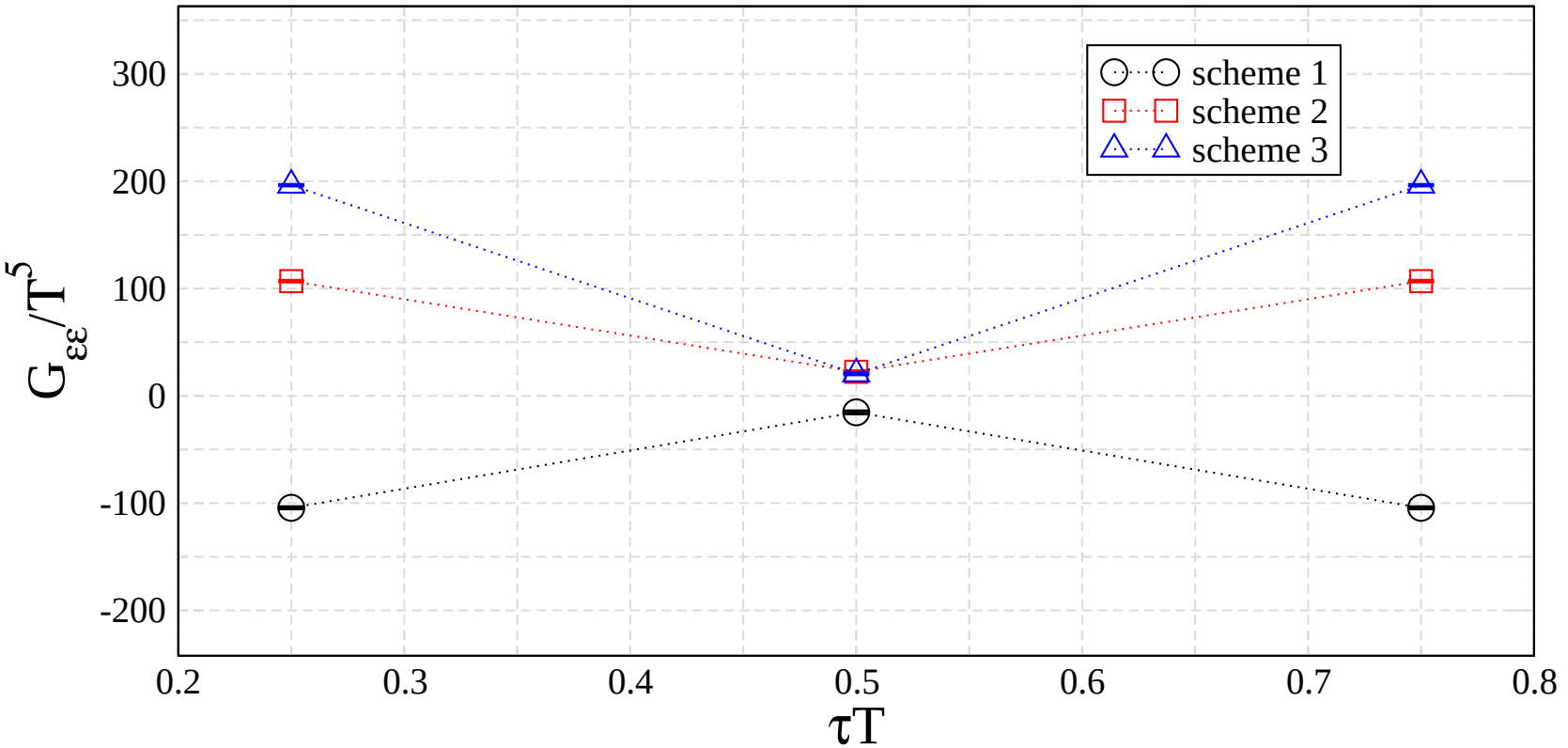

Discretization errors – larger N_τ

To better understand the magnitude of cut-off effects in the correlation functions, we performed some new simulations at larger $N_\tau = 6, 8$, $N_\sigma / N_\tau = 12$.
From the comparison at different N_τ of the three different discretization schemes, they seem to approach each other, even if the convergence is slow.

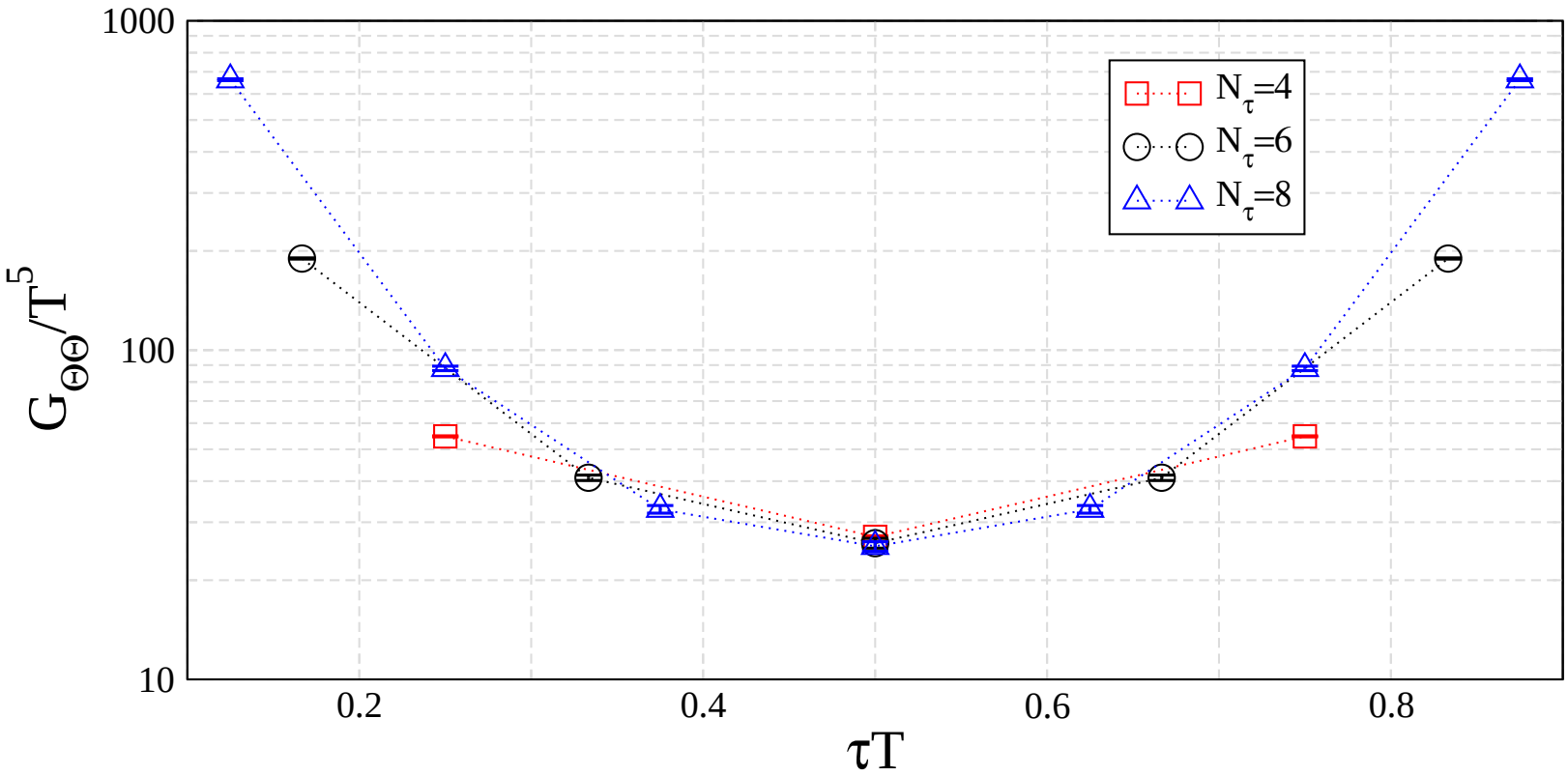

Discretization errors – larger N_τ

To better understand the magnitude of cut-off effects in the correlation functions, we performed some new simulations at larger $N_\tau = 6, 8$, $N_\sigma / N_\tau = 12$.
From the comparison at different N_τ of the three different discretization schemes, they seem to approach each other, even if the convergence is slow.

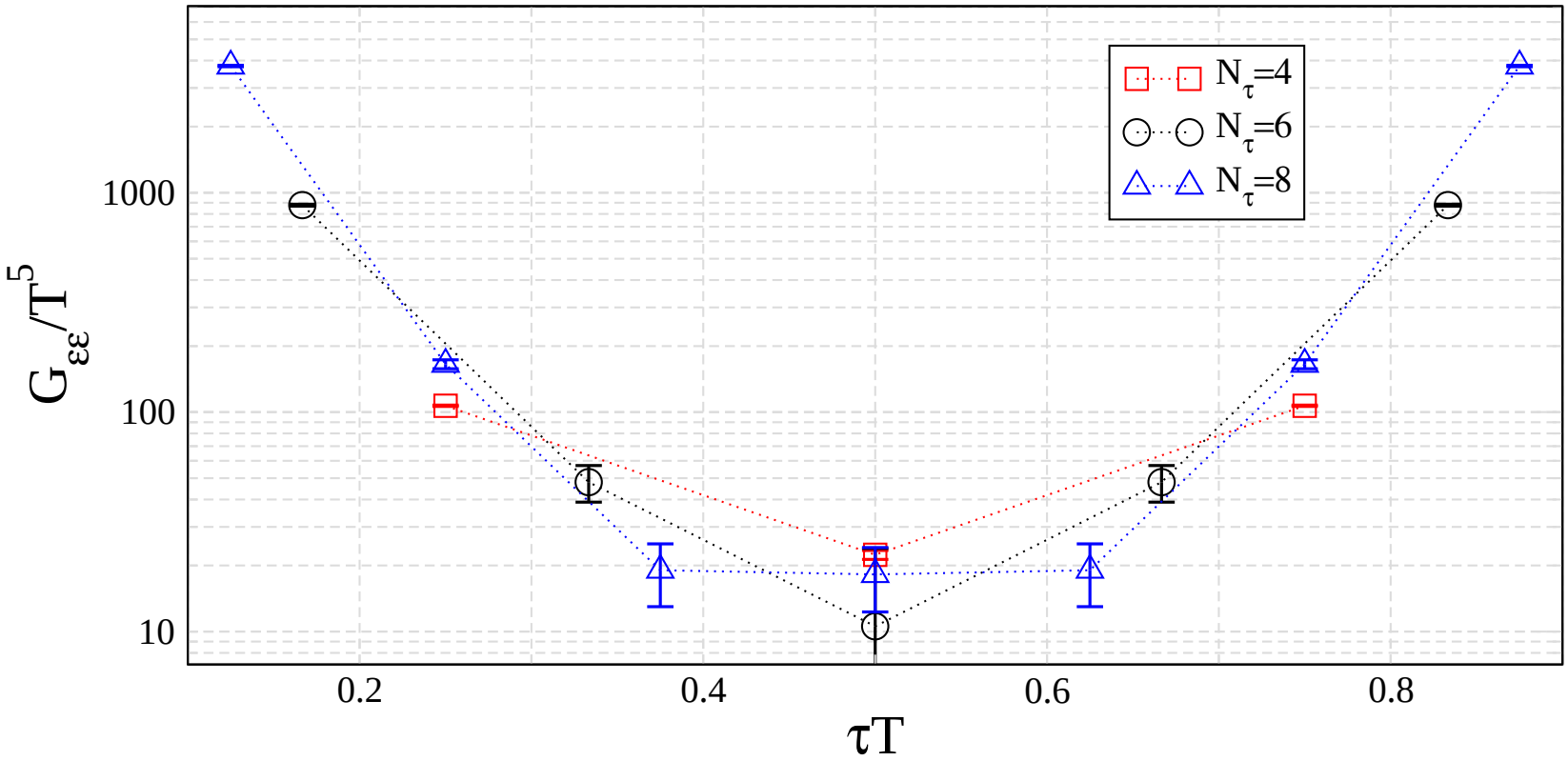

Discretization errors – larger N_τ

To better understand the magnitude of cut-off effects in the correlation functions, we performed some new simulations at larger $N_\tau = 6, 8$, $N_\sigma / N_\tau = 12$.
From the comparison at different N_τ of the three different discretization schemes, they seem to approach each other, even if the convergence is slow.

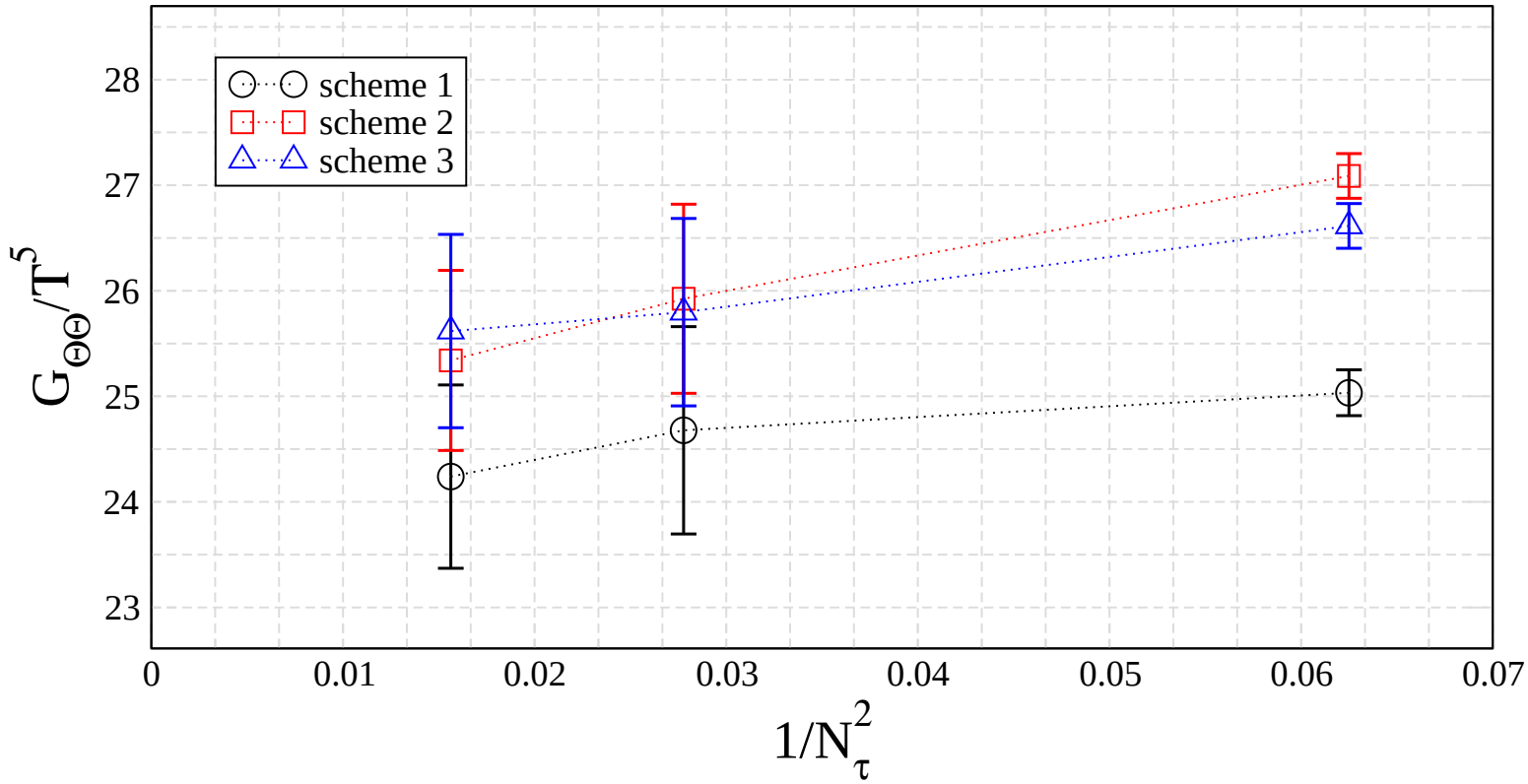

Discretization errors – larger N_τ

To better understand the magnitude of cut-off effects in the correlation functions, we performed some new simulations at larger $N_\tau = 6, 8$, $N_\sigma / N_\tau = 12$.
From the comparison at different N_τ of the three different discretization schemes, they seem to approach each other, even if the convergence is slow.

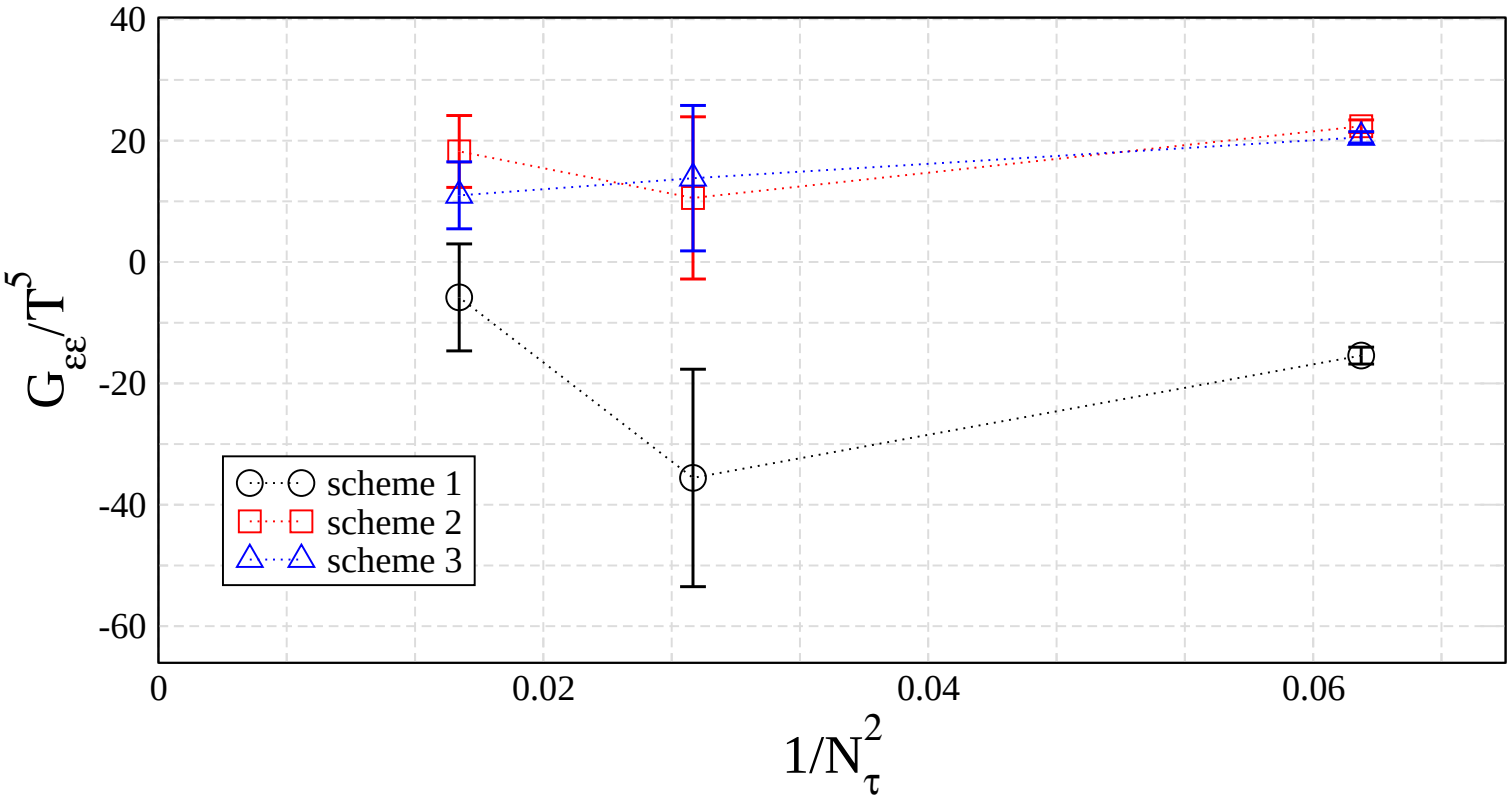

Discretization errors – larger N_τ

To better understand the magnitude of cut-off effects in the correlation functions, we performed some new simulations at larger $N_\tau = 6, 8$, $N_\sigma / N_\tau = 12$.
From the comparison at different N_τ of the three different discretization schemes, they seem to approach each other, even if the convergence is slow.

A better control of cut-off effects is highly desirable to make contact with the continuum correlation functions.

Discretization errors – critical behavior

On coarse lattices one may be worried about cut-off effects. Fortunately, these are not crucial for the analysis of critical behavior reflected by these correlation functions in the vicinity of the deconfinement transition.

As the correlation length is large close to T_c thermal effects are not very sensitive to the underlying cut-off. The cut-off dependence, being a short distance or large momentum effect, is part of the smooth regular background that contributes to $G_{XY}(\tau, T)$.

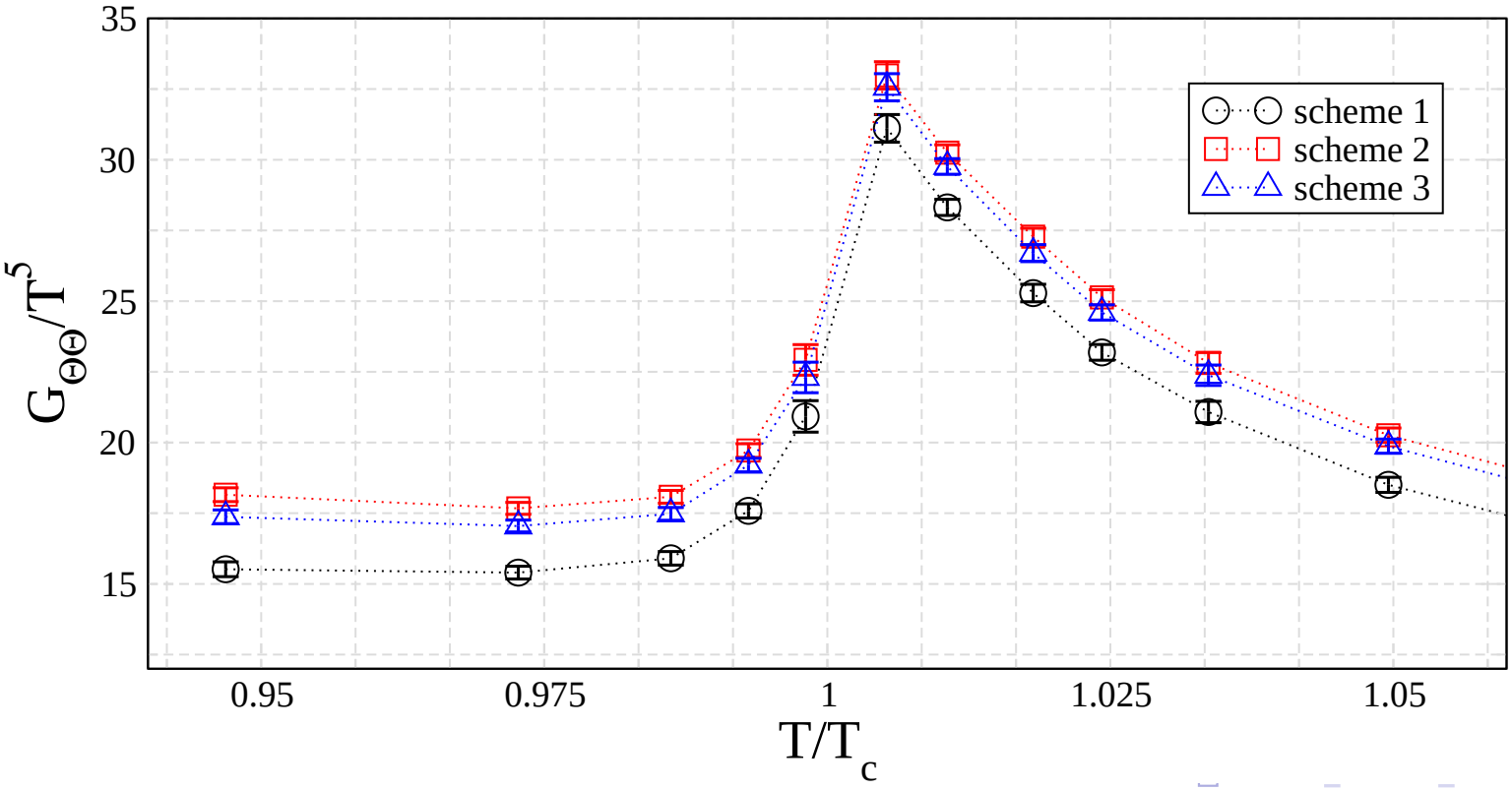

Discretization errors – critical behavior

On coarse lattices one may be worried about cut-off effects. Fortunately, these are not crucial for the analysis of critical behavior reflected by these correlation functions in the vicinity of the deconfinement transition.

As the correlation length is large close to T_c thermal effects are not very sensitive to the underlying cut-off. The cut-off dependence, being a short distance or large momentum effect, is part of the smooth regular background that contributes to $G_{XY}(\tau, T)$.